

Integrative Descriptions of Two New Macrobiotidae Species (Tardigrada: Eutardigrada: Macrobiotoida) from French Guiana and Malaysian Borneo

Daniel Stec^{1,*}, Magdalena Dudziak¹, and Łukasz Michalczyk¹

¹Institute of Zoology and Biomedical Research, Jagiellonian University, Gronostajowa 9, 30-387 Kraków, Poland.

*Correspondence: E-mail: daniel_stec@interia.eu (Stec)

E-mail: magdalena.dudziak@uj.edu.pl (Dudziak); LM@tardigrada.net (Michalczyk)

Received 27 March 2020 / Accepted 12 May 2020 / Published 2 July 2020
Communicated by Benny K.K. Chan

In this paper we describe two new tardigrade species, one representing the *Macrobiotus hufelandi* complex and the other from the *Paramacrobiotus richtersi* complex. The descriptions are based on a detailed morphological examination under light and scanning electron microscopy and analysis of four genetic markers (18S rRNA, 28S rRNA, ITS-2 and *COI*). *Macrobiotus crustulus* sp. nov. from French Guiana is the most similar to *Macrobiotus martini* Bartels, Pilato, Lisi and Nelson, 2009, *Macrobiotus santoroi* Pilato and D'Urso, 1976, but differs from them mainly by having the *lissostomus* type of the oral cavity armature (teeth not visible under light microscopy) and well-developed, convex terminal discs of egg processes covered with evident granulation. *Paramacrobiotus filipi* sp. nov. from the Malaysian part of Borneo is the most similar to *Paramacrobiotus alekseevi* (Tumanov, 2005), but differs from it primarily by the presence of body granulation visible under light microscopy as well as sculptured and porous areoles around egg processes.

Key words: Biodiversity, DNA barcodes, New species, Species complex, Taxonomy.

BACKGROUND

Tardigrades are a phylum of ubiquitous microinvertebrates that inhabit marine and limno-terrestrial environments throughout the world (Nelson et al. 2015). Currently, there are nearly 1300 formally recognised tardigrade species (Guidetti and Bertolani 2005; Degma and Guidetti 2007; Degma et al. 2009–2019). Although the great majority of species have been described classically, the number of taxa described under the integrative taxonomy framework is constantly increasing (e.g., Surmacz et al. 2019; Bochnak et al. 2020; Kayastha et al. 2020). Although studies on tardigrades have been conducted for more than two centuries, and have been particularly prevalent during

the last few decades, there are still regions of the world where these animals have never been studied. One such places is French Guiana, an overseas department of the French Republic located in the northern Atlantic coast of South America. Another part of the globe with weakly investigated tardigrade fauna is Malaysia where the only records come from its eastern part, Malaysian, Borneo, but with no reports from the peninsular part of the country. However, the Bornean tardigrade fauna is also very poorly known, as only four species from the island have been recorded so far: *Famelobiotus scalicii* Pilato, Binda and Lisi, 2004, *Bryodelphax arenosus* Gąsiorek, 2018, *Echiniscus masculinus* Gąsiorek, Vončina and Michalczyk, 2020 and *Insulobius orientalis* Gąsiorek and Michalczyk, 2020.

In this paper, we provide integrative descriptions of two new Macrobiotidae species, *Macrobiotus crustulus* sp. nov. from French Guiana and *Paramacrobiotus filipi* sp. nov. from the Malaysian part of Borneo. In addition, we also present new photomicrographs of the types of *Paramacrobiotus alekseevi* (Tumanov, 2005) and amend its description. The detailed morphological and morphometric data were obtained using light contrast and scanning electron microscopy. These data were further associated with DNA sequences of four genetic markers that are standard in modern tardigrade taxonomy (the nuclear 18S rRNA, 28S rRNA, and ITS-2, and the mitochondrial *COI*).

MATERIALS AND METHODS

The moss sample containing *Macrobiotus crustulus* sp. nov. was collected by Witold Morek and Bartłomiej Surmacz on 2 April 2019 from a tree trunk in the primeval tropical rainforest in the vicinity of Patawa, French Guiana, South America (4°33'58.2"N, 52°9'12.36"W; 268 m asl). The epiphyllous moss sample containing *Paramacrobiotus filipi* sp. nov. was collected by Piotr Gąsiorek on 27 July 2016 from the leaf of a tree in the primary tropical forest, Gunung Mulu, Sarawak, Borneo, Malaysia, Asia (4°02'N; 114°49'E; 100 m asl).

Both samples were examined for tardigrades using the protocol by Dastych (1980) with modifications described in detail in Stec et al. (2015). A total of 55 and 28 animals as well as 45 and 15 eggs of the two new species were extracted from the South American and Asian samples, respectively. In order to perform integrative taxonomic descriptions, the isolated animals and eggs were split into three groups for specific analyses: morphological analysis with phase contrast light microscopy (PCM), morphological analysis with scanning electron microscopy (SEM), and DNA sequencing (for details please see sections “Material examined” provided below for each description).

Microscopy and imaging

Specimens for light microscopy were mounted on microscope slides in a small drop of Hoyer's medium and secured with a cover slip, following the protocol by Morek et al. (2016). Slides were examined under an Olympus BX53 light microscopy, associated with an Olympus DP74 digital camera. Immediately after mounting the specimens in the medium, slides were also checked under PCM for the presence of males and females in the studied population as the spermatozoa in testis and spermathecae are visible for several hours

after mounting (Coughlan et al. 2019). In order to obtain clean and extended specimens for SEM, tardigrades were processed according to the protocol by Stec et al. (2015). Specimens were examined under high vacuum in a Versa 3D DualBeam Scanning Electron Microscope (SEM) at the ATOMIN facility of the Jagiellonian University, Kraków, Poland. All figures were assembled in Corel Photo-Paint X6, ver. 16.4.1.1281. For structures that could not be satisfactorily focused in a single PCM photograph, a stack of 2–6 images were taken with an equidistance of ca. 0.2 μm and assembled manually into a single deep-focus image in Corel Photo-Paint.

Morphometrics and morphological nomenclature

All measurements are given in micrometres (μm). Sample size was adjusted following recommendations by Stec et al. (2016). Structures were measured only if their orientation was suitable. Body length was measured from the anterior extremity to the end of the body, excluding the hind legs. The terminology used to describe oral cavity armature and egg shell morphology follows Michalczyk and Kaczmarek (2003) and Kaczmarek and Michalczyk (2017). The type of buccal apparatus and claws are given according to Pilato and Binda (2010). Macroplacoid length sequence is given according to Kaczmarek et al. (2014). Buccal tube length and the level of the stylet support insertion point were measured according to Pilato (1981). The *pt* index is the ratio of the length of a given structure to the length of the buccal tube, expressed as a percentage (Pilato 1981). All other measurements and nomenclature follow Kaczmarek and Michalczyk (2017). Morphometric data were handled using the “Parachela” ver. 1.7 template available from the Tardigrada Register (Michalczyk and Kaczmarek 2013). Raw morphometric data for each analysed species are provided as supplementary materials (Table S1 and Table S2) and are deposited in the Tardigrada Register under www.tardigrada.net/register/0068.htm (*M. crustulus* sp. nov.) and www.tardigrada.net/register/0069.htm (*P. filipi* sp. nov.). Tardigrade taxonomy follows Bertolani et al. (2014a).

Comparative material

First, to test whether our species had previously been described, we used dichotomous keys for the *Macrobiotus hufelandi* complex (Kaczmarek and Michalczyk 2017) and for the genus *Paramacrobiotus* (Kaczmarek et al. 2017). As they did not key to a recognised species, the specimens were compared with the original descriptions of the species most similar to them: *Macrobiotus martini* Bartels, Pilato, Lisi and

Nelson, 2009, *Macrobiotus santoroi* Pilato and D'Urso, 1976 and *Paramacrobiotus alekseevi* (Tumanov, 2005). Additionally, we used two slides containing a paratype and six eggs of *P. alekseevi* and new microphotographs of paratypes, which were kindly sent to us by Denis Tumanov (Saint-Petersburg State University, Russia).

Genotyping

Individual DNA extractions were made from eight specimens (four specimens per each new species) following protocol by Casquet et al. (2012) with modification presented by Stec et al. (2020c). Before the extraction, specimens were mounted in water, on temporary slides and checked under the microscope to confirm their identification. We sequenced four DNA fragments: the small ribosome subunit (18S

rRNA, nDNA), large ribosome subunit (28S rRNA, nDNA), internal transcribed spacer (ITS-2, nDNA), and cytochrome oxidase subunit I (*COI*, mtDNA). All fragments were amplified and sequenced according to the protocols described in Stec et al. (2020c); primers used in this study are listed in table 1. Sequencing products were read with the ABI 3130xl sequencer at the Molecular Ecology Lab, Institute of Environmental Sciences of the Jagiellonian University, Kraków, Poland. Sequences were processed in BioEdit ver. 7.2.5 (Hall 1999) and submitted to GenBank.

Comparative genetic analysis

For molecular comparisons, all published sequences of the four abovementioned markers for species of the *Macrobiotus hufelandi* complex and

Table 1. PCR primers for amplification of the four DNA fragments sequenced in the study

| DNA fragment | Primer name | Primer direction | Primer sequence (5'-3') | Primer source |
|--------------|-------------|------------------|----------------------------|------------------------|
| 18S rRNA | 18S_Tar_1Ff | forward | AGGCGAAACCGCGAATGGCTC | Stec et al. (2017a) |
| | 18S_Tar_1Rr | reverse | GCCGCAGGCTCCACTCCTGG | |
| 28S rRNA | 28S_Eutar_F | forward | ACCCGCTGAACTTAAGCATAT | Gąsiorek et al. (2018) |
| | 28SR0990 | reverse | CCTTGGTCCGTGTTTCAAGAC | Mironov et al. (2012) |
| ITS-2 | Eutar_Ff | forward | CGTAAACGTGAATTGCAGGAC | Stec et al. (2018a) |
| | Eutar_Rr | reverse | TCCTCCGCTTATTGATATGC | |
| <i>COI</i> | LCO1490 | forward | GGTCAACAAATCATAAAGATATTGG | Folmer et al. (1994) |
| | HCO2198 | reverse | TAAACTTCAGGGTGACCAAAAAATCA | |

Table 2. GenBank accession numbers for sequences of species of the *Macrobiotus hufelandi* complex analysed in this study. Underlined numbers indicate type and neotype sequences

| DNA marker | Species | Accession number | Source | |
|------------|-----------------------------------------------------------------------------------------|------------------|--------------------------|--------------------------|
| 18S rRNA | <i>M. canaricus</i> Stec et al., 2018 | <u>MH063925</u> | Stec et al. (2018b) | |
| | <i>M. engbergi</i> Stec et al., 2020 | <u>MN443039</u> | Stec et al. (2020a) | |
| | <i>M. noongaris</i> Coughlan and Stec, 2019 | <u>MK737069</u> | Coughlan and Stec (2019) | |
| | <i>M. kamilae</i> Coughlan and Stec, 2019 | <u>MK737070</u> | Coughlan and Stec (2019) | |
| | <i>M. caelestis</i> Coughlan et al., 2019 | <u>MK737073</u> | Coughlan et al. (2019) | |
| | " <i>M. hufelandi</i> " Schultzze, 1834 | GQ849024 | Giribet et al. (1996) | |
| | <i>M. hufelandi</i> group species | | HQ604971 | Bertolani et al. (2014a) |
| | | | FJ435738–40 | Guil and Giribet (2012) |
| | <i>M. hanna</i> e Nowak and Stec, 2018 | <u>MH063922</u> | Nowak and Stec (2018) | |
| | " <i>M. joannae</i> " Pilato and Binda, 1983 [= <i>M. hanna</i> e Nowak and Stec, 2018] | HQ604974–5 | Bertolani et al. (2014a) | |
| | <i>M. kristenseni</i> Guidetti et al., 2013 | <u>KC193577</u> | Guidetti et al. (2013) | |
| | <i>M. macrocalix</i> Bertolani and Rebecchi, 1993 | | <u>HQ604976</u> | Bertolani et al. (2014a) |
| | | | MH063926 | Stec et al. (2018b) |
| | <i>M. papei</i> Stec et al., 2018 | <u>MH063881</u> | Stec et al. (2018c) | |
| | <i>M. paulinae</i> Stec et al., 2015 | <u>KT935502</u> | Stec et al. (2015) | |
| | <i>M. polypiformis</i> Roszkowska et al., 2017 | <u>KX810008</u> | Roszkowska et al. (2017) | |
| | <i>M. polonicus</i> Pilato et al., 2003 | HM187580 | Welnicz et al. (2011) | |
| | <i>M. cf. recens</i> | MH063927 | Stec et al. (2018b) | |

Table 2. (Continued)

| DNA marker | Species | Accession number | Source |
|------------|---------------------------------------------------|-------------------------------------------------------------------|-----------------------------|
| | <i>M. sapiens</i> Binda and Pilato, 1984 | DQ839601 | Bertolani et al. (2014a) |
| | <i>M. scoticus</i> Stec et al., 2017 | KY797265 | Stec et al. (2017b) |
| | <i>M. shonaicus</i> Stec et al., 2018 | MG757132 | Stec et al. (2018d) |
| 28S rRNA | <i>M. canarius</i> Stec et al., 2018 | MH063934 | Stec et al. (2018b) |
| | <i>M. engbergi</i> Stec et al., 2020 | MN443034 | Stec et al. (2020a) |
| | <i>M. noongaris</i> Coughlan and Stec, 2019 | MK737063 | Coughlan and Stec (2019) |
| | <i>M. kamilae</i> Coughlan and Stec, 2019 | MK737064 | Coughlan and Stec (2019) |
| | <i>M. caelestis</i> Coughlan et al., 2019 | MK737071 | Coughlan et al. (2019) |
| | <i>M. hanna</i> e Nowak and Stec, 2018 | MH063924 | Nowak and Stec (2018) |
| | <i>M. hufelandi</i> group species | FJ435751, FJ435754–5 | Guil and Giribet (2012) |
| | <i>M. macrocalix</i> Bertolani and Rebecchi, 1993 | MH063935 | Stec et al. (2018b) |
| | <i>M. papei</i> Stec et al., 2018 | MH063880 | Stec et al. (2018c) |
| | <i>M. paulinae</i> Stec et al., 2015 | KT935501 | Stec et al. (2015) |
| | <i>M. polyipiformis</i> Roszkowska et al., 2017 | KX810009 | Roszkowska et al. (2017) |
| | <i>M. cf. recens</i> | MH063936 | Stec et al. (2018b) |
| | <i>M. scoticus</i> Stec et al., 2017 | KY797266 | Stec et al. (2017b) |
| | <i>M. shonaicus</i> Stec et al., 2018 | MG757133 | Stec et al. (2018d) |
| ITS-2 | <i>M. canarius</i> Stec et al., 2018 | MH063928–30 | Stec et al. (2018b) |
| | <i>M. engbergi</i> Stec et al., 2020 | MN443036–7 | Stec et al. (2020a) |
| | <i>M. noongaris</i> Coughlan and Stec, 2019 | MK737065–6 | Coughlan and Stec (2019) |
| | <i>M. kamilae</i> Coughlan and Stec, 2019 | MK737067 | Coughlan and Stec (2019) |
| | <i>M. caelestis</i> Coughlan et al., 2019 | MK737072 | Coughlan et al. (2019) |
| | <i>M. hanna</i> e Nowak and Stec, 2018 | MH063923 | Nowak and Stec (2018) |
| | <i>M. macrocalix</i> Bertolani and Rebecchi, 1993 | MH063931 | Stec et al. (2018b) |
| | <i>M. papei</i> Stec et al., 2018 | MH063921 | Stec et al. (2018c) |
| | <i>M. paulinae</i> Stec et al., 2015 | KT935500 | Stec et al. (2015) |
| | <i>M. polonicus</i> Pilato et al., 2003 | HM150647 | Welnicz et al. (2011) |
| | <i>M. polyipiformis</i> Roszkowska et al., 2017 | KX810010 | Roszkowska et al. (2017) |
| | <i>M. cf. recens</i> | MH063932–3 | Stec et al. (2018b) |
| | <i>M. sapiens</i> Binda and Pilato, 1984 | GQ403680 | Schill et al. (2010) |
| | <i>M. scoticus</i> Stec et al., 2017 | KY797268 | Stec et al. (2017b) |
| | <i>M. shonaicus</i> Stec et al., 2018 | MG757134–5 | Stec et al. (2018d) |
| COI | <i>M. canarius</i> Stec et al., 2018 | MH057765–6 | Stec et al. (2018b) |
| | <i>M. engbergi</i> Stec et al., 2020 | MN444824–6 | Stec et al. (2020a) |
| | <i>M. noongaris</i> Coughlan and Stec, 2019 | MK737919 | Coughlan and Stec (2019) |
| | <i>M. kamilae</i> Coughlan and Stec, 2019 | MK737920–1 | Coughlan and Stec (2019) |
| | <i>M. caelestis</i> Coughlan et al., 2019 | MK737922 | Coughlan et al. (2019) |
| | <i>M. hanna</i> e Nowak and Stec, 2018 | MH057764 | Nowak and Stec (2018) |
| | <i>M. cf. hufelandi</i> , Schultze, 1834 | HQ876589–94, HQ876596 | Bertolani et al. (2011a) |
| | <i>M. hufelandi</i> s.s., Schultze, 1834 | HQ876584 , HQ876586–8 | Bertolani et al. (2011a) |
| | <i>M. kristenseni</i> Guidetti et al., 2013 | KC193575–6 | Guidetti et al. (2013) |
| | <i>M. macrocalix</i> Bertolani and Rebecchi, 1993 | FJ176203–7 , FJ176208–17 | Cesari et al. (2009) |
| | | HQ876571 | Bertolani et al. (2011a) |
| | | MH057767 | Stec et al. (2018b) |
| | <i>M. papei</i> Stec et al., 2018 | MH057763 | Stec et al. (2018c) |
| | <i>M. paulinae</i> Stec et al., 2015 | KT951668 | Stec et al. (2015) |
| | <i>M. polyipiformis</i> Roszkowska et al., 2017 | KX810011–2 | Roszkowska et al. (2017) |
| | <i>M. cf. recens</i> | MH057768–9 | Stec et al. (2018b) |
| | <i>M. sandrae</i> Bertolani and Rebecchi, 1993 | HQ876566–67, HQ876569–70, HQ876572–83 | Bertolani et al. (2011a) |
| | <i>M. scoticus</i> Stec et al., 2017 | KY797267 | Stec et al. (2017b) |
| | <i>M. shonaicus</i> Stec et al., 2018 | MG757136–7 | Stec et al. (2018d) |
| | <i>M. terminalis</i> Bertolani and Rebecchi, 1993 | JN673960 | Cesari et al. (2011) |
| | | AY598775 | Guidetti et al. (2005) |
| | <i>M. vladimiri</i> Bertolani et al., 2011 | HM136931–2 , HM136933–4, HQ876568 | Bertolani et al. (2011a, b) |

the genus *Paramacrobotus* were downloaded from GenBank (Tables 2 and 3). The sequences were aligned using the default settings (in the case of the ITS-2 and *COI*) and the Q-INS-I method (in the case of the ribosomal markers: 18S rRNA, 28S rRNA) of MAFFT version 7 (Katoh et al. 2002; Katoh and Toh 2008) and manually checked against non-conservative alignments in BioEdit. Then, the aligned sequences were trimmed to: 763 (18S rRNA), 715 (28S rRNA), 426 (ITS-2), and 624 (*COI*) bp for *Macrobotus hufelandi* complex and 766 (18S rRNA), 727 (28S rRNA), and 588 (*COI*) bp for the genus *Paramacrobotus*. All *COI* sequences were translated into protein sequences in MEGA7 version

7.0 (Kumar et al. 2016) to check against pseudogenes. Uncorrected pairwise distances were calculated using MEGA7 and are provided as supplementary materials (Table S3).

RESULTS

TAXONOMY

Phylum Tardigrada Doyère, 1840
Class Eutardigrada Richters, 1926
Order Parachela Schuster, Nelson, Grigarick

Table 3. GenBank accession numbers for sequences of *Paramacrobotus* species analysed in this study. Underlined numbers indicate type or neotype sequences

| DNA marker | Species | Accession number | Source |
|-------------------------------------------------|-------------------------------------------------|-------------------------------------------------------------------------------------------------------------------------|-------------------------------------------------------------------------------------------------|
| 18S rRNA | <i>P. areolatus</i> s.s. (Murray, 1907) | <u>MH664931</u> | Stec et al. (2020b) |
| | <i>P. lachowskiae</i> Stec et al., 2018 | <u>MF568532</u> | Stec et al. (2018e) |
| | <i>P. fairbanksi</i> Schill et al., 2010 | MH664941–42, MK041027–9 | Stec et al. (2020b), Guidetti et al. 2019 |
| | <i>P. tonollii</i> (Ramazzotti, 1956) | MH664946, DQ839605 | Stec et al. (2020b), Guidetti et al. 2009 |
| | <i>P. richtersi</i> s.s. (Murray, 1911) | <u>MK041023</u> | Guidetti et al. (2019) |
| | <i>P. spatialis</i> Guidetti et al., 2019 | <u>MK041024–6</u> | Guidetti et al. (2019) |
| | <i>P. depressus</i> Guidetti et al., 2019 | <u>MK041030</u> | Guidetti et al. (2019) |
| | <i>P. celsus</i> Guidetti et al., 2019 | <u>MK041031</u> | Guidetti et al. (2019) |
| | <i>P. arduus</i> Guidetti et al., 2019 | <u>MK041032</u> | Guidetti et al. (2019) |
| | <i>P. experimentalis</i> Kaczmarek et al., 2020 | <u>MN073467–8</u> | Kaczmarek et al. (2020) |
| | <i>P. areolatus</i> group species | MH664937, MH664943, DQ839602 | Stec et al. (2020b), Guidetti et al. (2009) |
| | <i>P. richtersi</i> group species | MH664932–6, MH664938–40, MH664944–5, HQ604985–6, EU038078, EU038080–1, DQ839603 | Stec et al. (2020b) Bertolani et al. (2014a) Guidetti et al. (2009) |
| | 28S rRNA | <i>P. areolatus</i> s.s. (Murray, 1907) | <u>MH664948</u> |
| <i>P. lachowskiae</i> Stec et al., 2018 | | <u>MF568533</u> | Stec et al. (2018e) |
| <i>P. fairbanksi</i> Schill et al., 2010 | | MH664950, MH664959 | Stec et al. (2020b) |
| <i>P. tonollii</i> (Ramazzotti, 1956) | | MH664963 | Stec et al. (2020b) |
| <i>P. experimentalis</i> Kaczmarek et al., 2020 | | <u>MN073465–6</u> | Kaczmarek et al. (2020) |
| <i>P. areolatus</i> group species | | MH664955, MH664960 | Stec et al. (2020b) |
| <i>P. richtersi</i> group species | | MH664949, MH664951–4, MH664956–8, MH664961–2, FJ435757 | Stec et al. (2020b), Guil and Giribet (2012) |
| <i>COI</i> | | <i>P. areolatus</i> (Murray, 1907) | <u>MH675998</u> |
| | <i>P. lachowskiae</i> Stec et al., 2018 | <u>MF568534</u> | Stec et al. (2018e) |
| | <i>P. fairbanksi</i> Schill et al., 2010 | MH676011–2, <u>EU244597</u> , FJ435808–9, MK041003–11, AY598778–9 | Stec et al. (2020b), Guidetti et al. (2005), Guidetti et al. (2019), Guil and Giribet (2012) |
| | <i>P. tonollii</i> (Ramazzotti, 1956) | MH676018 | Stec et al. (2020b) |
| | <i>P. richtersi</i> (Murray, 1911) | <u>MK040992–4</u> | Guidetti et al. (2019) |
| | <i>P. spatialis</i> Guidetti et al., 2019 | <u>MK040995–9</u> , <u>MK041000–2</u> | Guidetti et al. (2019) |
| | <i>P. depressus</i> Guidetti et al., 2019 | <u>MK041012–6</u> | Guidetti et al. (2019) |
| | <i>P. celsus</i> Guidetti et al., 2019 | <u>MK041017–9</u> | Guidetti et al. (2019) |
| | <i>P. arduus</i> Guidetti et al., 2019 | <u>MK041020–22</u> | Guidetti et al. (2019) |
| | <i>P. experimentalis</i> Kaczmarek et al., 2020 | <u>MN097836–37</u> | Kaczmarek et al. (2020) |
| | <i>P. areolatus</i> group species | <u>MH676007</u> , <u>MH676013</u> | Stec et al. (2020b) |
| | <i>P. richtersi</i> group species | <u>MH675999</u> , <u>MH676000–6</u> , <u>MH676008–10</u> , <u>MH676014–7</u> , <u>EU244598–9</u> , <u>KF788251–7</u> | Stec et al. (2020b), Guidetti et al. (2009), Caicedo et al. (2017) |

and Christenberry, 1980
Superfamily Macrobitoidea Thulin, 1928 (in
Marley et al. 2011)
Family Macrobiotidae Thulin, 1928
Genus *Macrobiotus* C.A.S. Schultze, 1834

***Macrobiotus crustulus* sp. nov. Stec, Dudziak & Michalczyk**

(Figs. 1–8, Tables 2–3)

urn:lsid:zoobank.org:act:F6723AE7-2F15-4FEA-A6BC-76C3B48AE1C1

Material examined: 55 animals and 45 eggs. Specimens mounted on microscope slides in Hoyer's medium (50 animals + 44 eggs), fixed on SEM stubs (1 + 1), and processed for DNA sequencing (4 + 0).

Type locality: 4°33'58.2"N, 52°9'12.36"W; 268 m asl: French Guiana: the vicinity of Patawa; moss on the tree trunk in primeval tropical rainforest; coll. 2 April 2018 by Witold Morek and Bartłomiej Surmacz.

Type depositories: Holotype (slide GF.271.06 with 4 paratypes) and 46 paratypes (slides: GF.271.* , where the asterisk can be substituted by any of the following numbers 01–05, 07–09; SEM stub: 19.16) and 45 eggs (slides: GF.271.*: 10–16; SEM stub: 19.16) are deposited at the Institute of Zoology and Biomedical Research, Jagiellonian University, Gronostajowa 9, 30-387, Kraków, Poland.

Etymology: The name refers to morphology of terminal discs of processes on the egg shell that resemble oat cookies. From Latin “cookie” = “*crustulum*”.

Description: Animals (measurements and statistics in Table 4). Body transparent in juveniles and whitish in adults, after fixation in Hoyer's medium – transparent (Fig. 1A). Eyes present, visible also in specimens mounted in Hoyer's medium. Cuticle porous with circular and elliptical pores (diameter range: 0.8–2.4 µm) clearly visible on the entire body (Fig. 1B–C). Patches of granulation on all legs present and visible under PCM as singular dots/granules whereas under SEM these dots are revealed as aggregations of smaller microgranules (Fig. 2A–F). A patch of clearly visible granulation is present on the external surface of legs I–III (Fig. 2A–B). A pulvinus is present on the internal surface of legs I–III, together with faint granulation situated below the pulvinus (Fig. 2C–D). Granulation on legs IV is always visible and consists of a single large granulation patch on each leg covering dorsal and lateral leg surfaces (Fig. 2E–F).

Claws stout, of the *hufelandi* type (Fig. 3A–D). Primary branches with distinct accessory points, a common tract, and with an evident stalk connecting the claw to the lunula (Fig. 3A–D). Lunulae on all legs

smooth (Fig. 3A–D). Cuticular bars under claws are absent. Double muscle attachments are faintly marked in PCM (Fig. 3A).

Mouth antero-ventral followed by ten short peribuccal lamellae (Fig. 5A–B), bucco-pharyngeal apparatus of the *Macrobiotus* type with thickened walls of the buccal tube posterior to the stylets support insertion point (Figs. 4A, 5A–B). Under PCM, the oral cavity armature is of the *lissostomus* type, *i.e.*, teeth in the oral cavity not visible (Fig. 4B–C). However, in SEM, two bands of teeth are clearly visible with the first band being situated at the base of peribuccal lamellae and composed of a 4–6 rows of small cone-shaped/granular teeth arranged around the oral cavity (Fig. 5A–B). The second band of teeth is situated behind the ring fold and comprises 4–6 rows of small cone-shaped/granular teeth which are larger than those of the first band (Fig. 5A–B). The teeth of the third band are reduced to irregular wrinkled cuticular thickenings posterior to the second band of teeth (Fig. 5A–B). Pharyngeal bulb spherical, with triangular apophyses, two rod-shaped macroplacoids and a triangular small microplacoid (Fig. 4A, D–E). The macroplacoid length sequence $2 < 1$. The first macroplacoid has a central constriction whereas the second macroplacoid is constricted subterminally (Fig. 4D–E).

Eggs (measurements and statistics in Table 5): Laid freely, whitish, spherical (Figs. 6A, 7A). The surface between the processes is of the *hufelandi* type, *i.e.*, covered with a reticulum with very thin walls (Figs. 6F–G, 7A–F). Peribasal meshes of similar size compared to interbasal meshes, usually with three to four rows of meshes between the neighbouring processes (Figs. 6F–G, 7A–F). Mesh diameter is always larger than mesh walls and nodes (Figs. 6F–G, 7A–F). The meshes are 0.7–1.6 µm in diameter, polygonal but with rounded edges. In SEM, meshes deep and empty inside and the whole reticulum is gently attached to the chorion surface by faint connectors what makes the impression that the reticulum is hanging over the egg surface (Fig. 7B–F). Processes are of the inverted goblet shape with slightly concave trunks but convex terminal discs (Figs. 6A–C, 7A–D). The central portion of each processes trunk is covered by small granulation that is visible only under SEM (Fig. 7B–E) Terminal discs are round with serrated/jagged edges and with a convex central area covered by a uniformly distributed granulation visible clearly both in PCM and SEM (Figs. 6B–E, 7A–D).

Reproduction: The new species is dioecious. Spermathecae in females as well as testis in males have been found to be filled with spermatozoa, clearly visible under PCM up to 24 hours after mounting in Hoyer's medium (Fig. 8A–D). The new species does not exhibit

secondary sexual dimorphism (e.g., males do not have gibbosities on hind legs).

DNA sequences: We obtained sequences for all four of the above mentioned DNA markers, each of which was represented by a single haplotype: 18S rRNA sequence (GenBank: MT261912), 1014 bp long; 28S rRNA sequence (GenBank: MT261903), 720 bp long; ITS-2 sequence (GenBank: MT261907), 439 bp long; COI sequence (GenBank: MT260371), 658 bp long.

Remarks: *Macrobotus crustulus* sp. nov. is the first ever tardigrade species reported from French Guiana.

Genus: *Paramacrobotus* Guidetti, Schill, Bertolani, Dandekar and Wolf, 2009.

***Paramacrobotus filipi* sp. nov. Dudziak, Stec & Michalczyk**

(Figs. 9–13, Tables 4–5)

urn:lsid:zoobank.org:act:EED1679C-D91B-4D9A-B4CB-21E6B50180C9

Material examined: 28 animals and 15 eggs. Specimens mounted on microscope slides in Hoyer’s medium (24 animals + 10 eggs), fixed on SEM stubs (0+5), and processed for DNA sequencing (4+0).

Type locality: 44°02’N, 114°49’E; 100 m asl: Malaysia: Sarawak, Borneo, Gunung Mulu; epiphyllous moss on the tree leaf in the primary tropical forest; coll. 27 July 2016 by Piotr Gąsiorek.

Table 4. Measurements [in µm] of selected morphological structures of *Macrobotus crustulus* sp. nov. individuals mounted in Hoyer’s medium

| Character | N | Range | | Mean | | SD | | Holotype | |
|--------------------------------|----|-----------|-----------|------|------|-----|-----|----------|------|
| | | µm | pt | µm | pt | µm | pt | µm | pt |
| Body length | 22 | 238–567 | 767–1242 | 379 | 1000 | 82 | 126 | 490 | 1029 |
| Buccal tube | | | | | | | | | |
| Buccal tube length | 22 | 29.1–47.6 | – | 37.5 | – | 4.5 | – | 47.6 | – |
| Stylet support insertion point | 22 | 20.7–33.2 | 69.3–72.7 | 26.7 | 71.2 | 3.2 | 1.2 | 33.0 | 69.3 |
| Buccal tube external width | 22 | 2.7–5.3 | 9.3–12.7 | 4.1 | 10.8 | 0.6 | 0.9 | 4.8 | 10.1 |
| Buccal tube internal width | 22 | 1.6–2.7 | 5.1–6.5 | 2.1 | 5.7 | 0.3 | 0.4 | 2.5 | 5.3 |
| Ventral lamina length | 22 | 14.0–22.4 | 46.9–55.8 | 18.9 | 50.6 | 2.0 | 2.9 | 22.4 | 47.1 |
| Placoid lengths | | | | | | | | | |
| Macroplacoid 1 | 22 | 6.9–14.5 | 23.6–31.7 | 10.4 | 27.7 | 1.8 | 2.3 | 13.0 | 27.3 |
| Macroplacoid 2 | 22 | 4.6–11.0 | 15.8–23.1 | 7.4 | 19.5 | 1.5 | 2.0 | 11.0 | 23.1 |
| Microplacoid | 22 | 2.0–3.6 | 4.8–9.0 | 2.6 | 6.8 | 0.4 | 1.0 | 3.6 | 7.6 |
| Macroplacoid row | 22 | 13.4–25.0 | 46.0–57.0 | 19.4 | 51.4 | 3.1 | 2.8 | 25.0 | 52.5 |
| Placoid row | 22 | 16.2–28.9 | 55.7–61.2 | 22.1 | 58.7 | 3.1 | 1.7 | 28.9 | 60.7 |
| Claw 1 heights | | | | | | | | | |
| External primary branch | 21 | 7.6–12.6 | 22.4–31.2 | 9.8 | 26.5 | 1.3 | 2.1 | 12.6 | 26.5 |
| External secondary branch | 20 | 5.7–10.1 | 16.9–24.7 | 7.8 | 20.9 | 1.2 | 2.1 | 10.1 | 21.2 |
| Internal primary branch | 21 | 7.1–12.8 | 22.3–28.2 | 9.6 | 25.4 | 1.4 | 1.6 | 12.8 | 26.9 |
| Internal secondary branch | 19 | 4.9–10.7 | 16.8–23.4 | 7.5 | 19.8 | 1.4 | 1.5 | 10.3 | 21.6 |
| Claw 2 heights | | | | | | | | | |
| External primary branch | 22 | 7.3–12.6 | 22.6–29.5 | 9.9 | 26.4 | 1.3 | 1.7 | 12.6 | 26.5 |
| External secondary branch | 22 | 5.1–10.1 | 17.5–23.5 | 7.8 | 20.6 | 1.2 | 1.6 | 10.1 | 21.2 |
| Internal primary branch | 22 | 7.1–12.8 | 23.9–29.7 | 9.8 | 26.0 | 1.5 | 1.5 | 12.8 | 26.9 |
| Internal secondary branch | 21 | 5.6–10.4 | 17.9–23.5 | 7.9 | 20.7 | 1.2 | 1.6 | 10.4 | 21.8 |
| Claw 3 heights | | | | | | | | | |
| External primary branch | 19 | 7.2–12.5 | 21.9–28.5 | 10.0 | 26.2 | 1.4 | 1.5 | 12.5 | 26.3 |
| External secondary branch | 20 | 5.2–10.3 | 16.3–23.7 | 7.8 | 20.5 | 1.2 | 1.7 | 10.3 | 21.6 |
| Internal primary branch | 20 | 7.1–12.8 | 21.8–28.2 | 9.6 | 25.4 | 1.4 | 1.6 | 12.8 | 26.9 |
| Internal secondary branch | 18 | 5.4–10.7 | 16.1–23.3 | 7.7 | 20.1 | 1.2 | 1.7 | 10.7 | 22.5 |
| Claw 4 heights | | | | | | | | | |
| Anterior primary branch | 20 | 7.2–15.5 | 24.7–33.3 | 11.3 | 30.1 | 2.0 | 2.5 | 15.5 | 32.6 |
| Anterior secondary branch | 18 | 6.7–13.3 | 20.1–30.5 | 9.0 | 23.7 | 1.7 | 2.4 | 12.1 | 25.4 |
| Posterior primary branch | 18 | 8.3–15.3 | 25.7–33.8 | 11.8 | 31.0 | 1.8 | 2.3 | 15.3 | 32.1 |
| Posterior secondary branch | 12 | 6.8–10.2 | 19.1–27.0 | 8.9 | 24.4 | 1.1 | 2.3 | ? | ? |

N, number of specimens/structures measured; Range, refers to the smallest and the largest structure among all measured specimens; SD, standard deviation.

Type depositories: Holotype (slide MY.098.01 with 4 paratypes) and 19 paratypes (slides: MY.098.*, where the asterisk can be substituted by any of the following numbers 02, 04–05) and 15 eggs (slides: MY.098.*: 03, 06; SEM stub: 18.13) are deposited at

the Institute of Zoology and Biomedical Research, Jagiellonian University, Gronostajowa 9, 30-387, Kraków, Poland.

Etymology: We take great pleasure in dedicating this new species to Filip Dudziak, son of the second

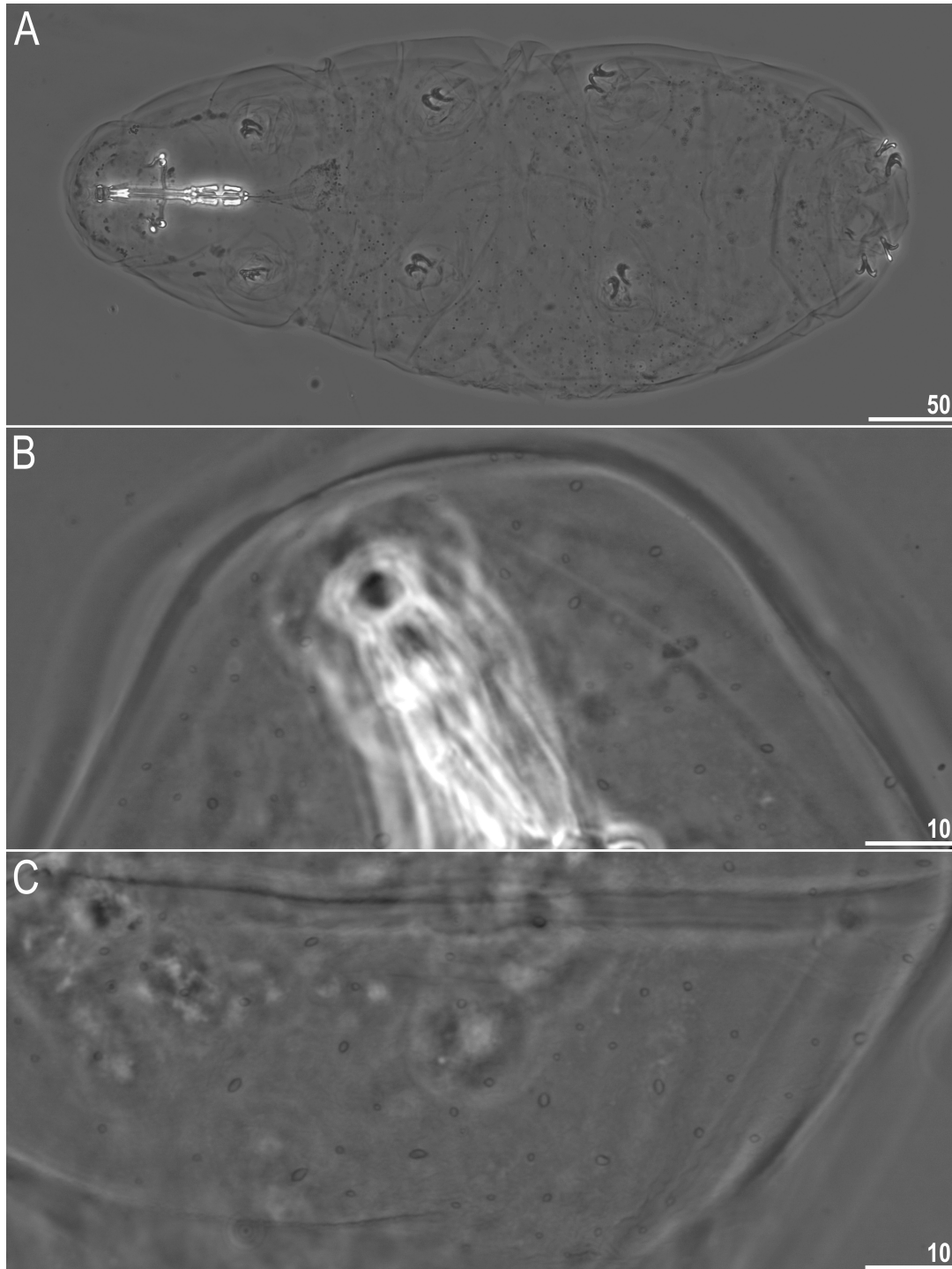


Fig. 1. *Macrobotus crustulus* sp. nov., habitus and cuticular pores (PCM). A, dorso-ventral projection (holotype, Hoyer's medium); B–C, cuticular pores on the dorso-cephalic (B) and dorso-caudal (C) part of the body. Scale bars in μm .

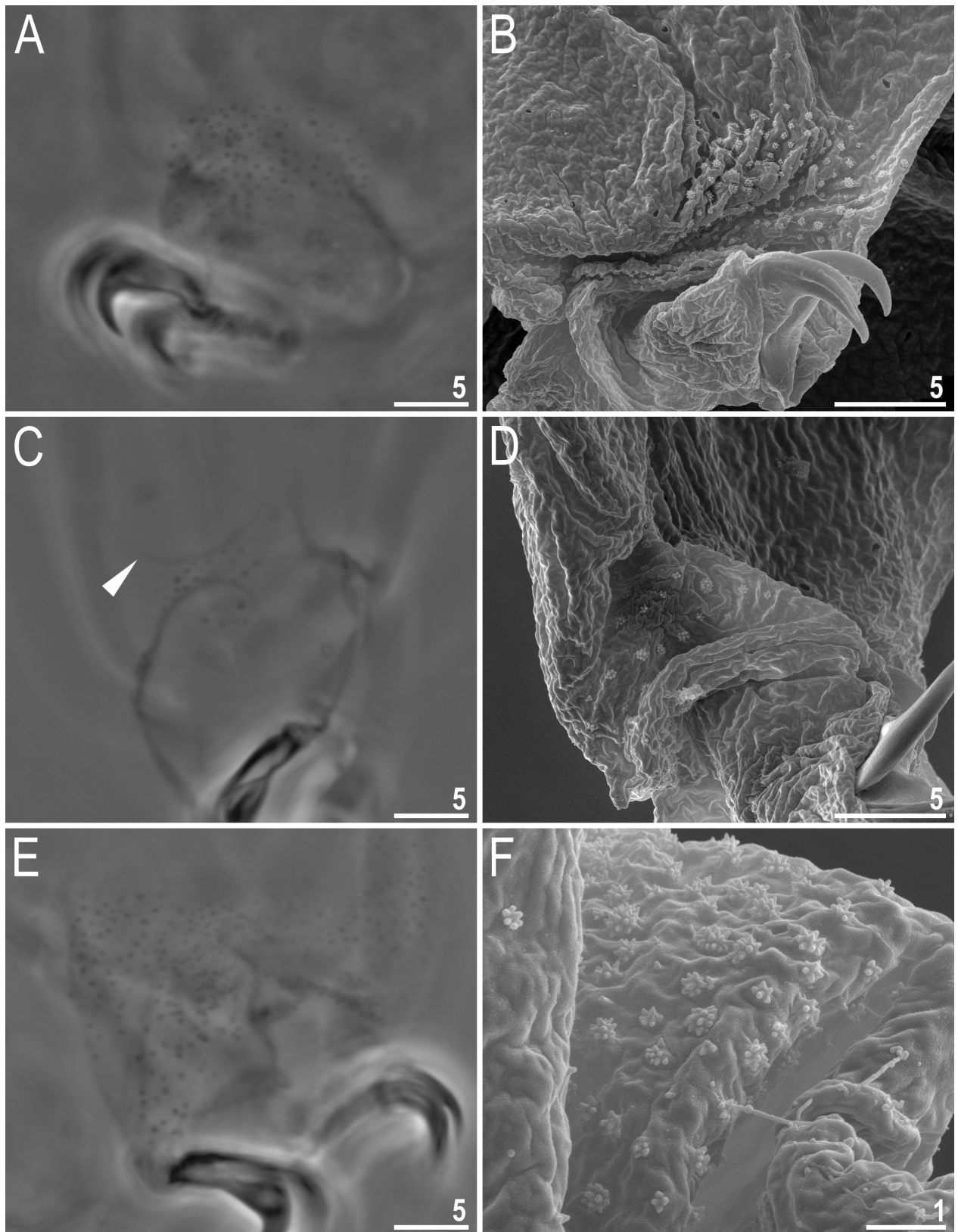


Fig. 2. *Macrobiotus crustulus* sp. nov., cuticular structures on legs (paratypes). A–B, external granulation on leg II seen in PCM (A) and SEM (B), respectively; C–D, a cuticular bulge (pulvinus) and a faint granulation, on the internal surface of legs I and II seen in PCM (C) and SEM (D), respectively; E–F, granulation on leg IV seen in PCM (E) and SEM (F). Filled flat arrowheads indicate the pulvinus. Scale bars in μm .

author.

Description: Animals (measurements and statistics in Table 4): Before mounting in Hoyer’s medium, body almost transparent in juveniles and white in adults, eyes absent; after fixation on microscope slides body transparent (Fig. 9A). Body cuticle covered with fine granulation clearly visible on the dorsal side of the caudal body region (Fig. 9B). On legs I–III, a patch of fine granulation is placed on the external surface of the legs, near the claws (Fig. 9C), whereas granulation on legs IV extends from the claws onto the entire dorsolateral surface of the legs, being denser towards the claws (Fig. 9E). A pulvinus is present on the internal surface of legs I–III (Fig. 9D).

Claws slender, of the *hufelandi* type. Primary

branches with distinct accessory points, a long common tract, and with an evident stalk connecting the claw to the lunula (Fig. 10A–B). Lunulae on all legs smooth (Fig. 10A–B). Bars under claws absent (Fig. 10A–B).

Mouth antero-ventral, bucco-pharyngeal apparatus of the *Macrobotus* type (Fig. 11A). The oral cavity armature well-developed and composed of three bands of teeth (Fig. 11B–E). The first band of teeth comprises numerous small granules arranged in a several rows situated anteriorly in the oral cavity, just behind the bases of the peribuccal lamellae (Fig. 11B–E). The second band of teeth is situated between the ring fold and the third band of teeth, and is composed of ridges parallel to the main axis of the buccal tube (Fig. 11B–E). The teeth of the third band are located within the

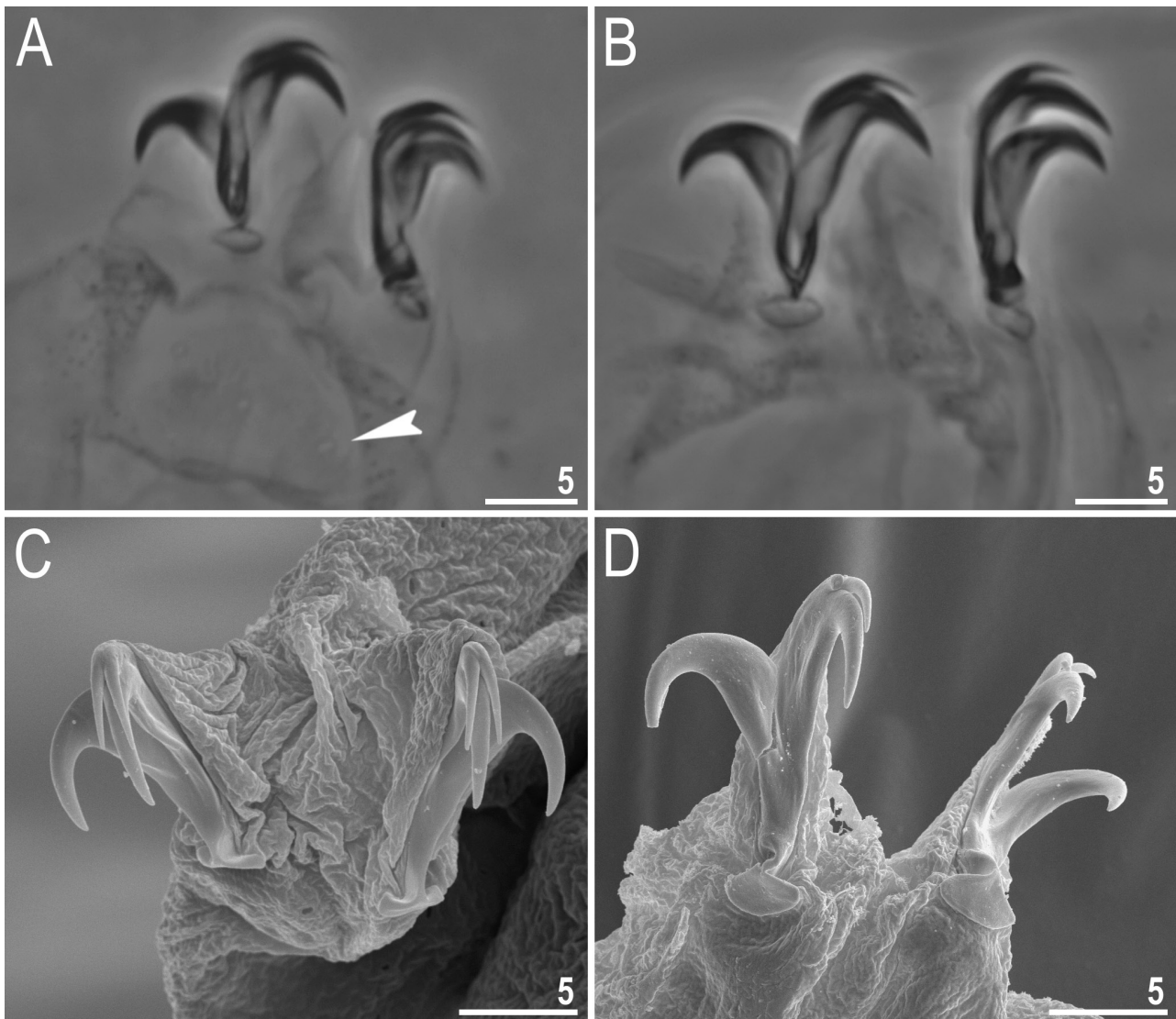


Fig. 3. *Macrobotus crustulus* sp. nov., claws (paratypes). A–B, claws III (A) and IV (B) seen in PCM; C–D, claws I (C) and IV (D) seen in SEM. Filled flat arrowheads indicate double muscle attachments under the claws. Scale bars in µm.

posterior portion of the oral cavity, between the second band of teeth and the buccal tube opening (Fig. 11B–E). The third band of teeth is divided into the dorsal and the ventral portion. Under PCM, both dorsal and ventral teeth are visible as two lateral and one median

transverse ridges (Fig. 11B–E). The ventro-median tooth is divided into two roundish teeth of which one is sometimes larger (Fig. 11C, E). Pharyngeal bulb spherical, with triangular apophyses, three rod-shaped macroplacoids and a microplocoid clearly distant (more

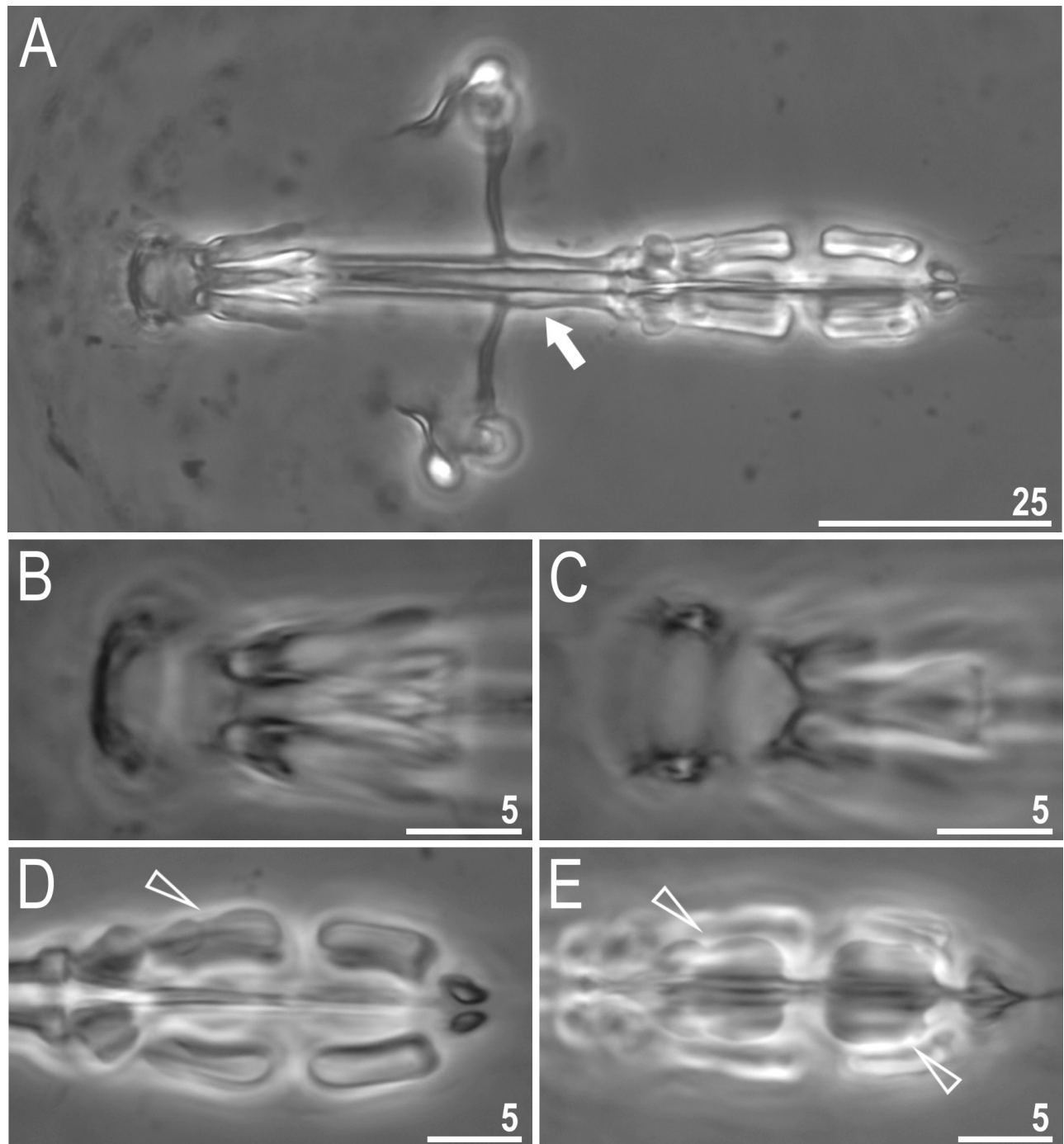


Fig. 4. *Macrobotus crustulus* sp. nov., buccal apparatus and the oral cavity armature seen in PCM. A, dorso-ventral projection of the buccal apparatus (holotype); B–C, oral cavity armature of the *lissostomus* type (*i.e.*, no bands of teeth visible under PCM), dorsal (B) and ventral (C) view (paratype); D–E, placoid morphology, dorsal (D) and ventral (E) view (paratype). The arrow indicates thickened walls of the buccal tube posterior to the stylet support insertion point, empty arrowheads indicate constrictions in macroplacoids. Scale bars in μm .

than its length) from the third macroplacoid (Fig. 11A, F–G). The macroplacoid length sequence is $2 < 1 < 3$. The first macroplacoid is anteriorly narrowed and the third has a subterminal constriction (Fig. 11F–G).

Eggs (measurements and statistics in Table 5): Laid freely, white, spherical with conical processes with the elongated terminal portion terminated with a small concave disc with an irregular edge (Figs. 12A–F, 13A–F). The labyrinthine layer between the process walls is visible under PCM as a reticular pattern with slightly sinuous margins (Fig. 12A–B). Eight to ten areoles are present around each process (Figs. 12A–B, 13A–B). The surface of the areoles is sculptured and porous (Figs. 12A–B, 13A–D). Pores large and visible both under PCM and SEM (Figs. 12A–B, 13A–D, respectively). The ridges separating each areole are narrower than the

areole diameter (Figs. 12A–B, 13A–D).

Reproduction: The new species is probably parthenogenetic since no spermathecae or testis filled with spermatozoa were found in specimens freshly mounted in Hoyer’s medium.

DNA sequences: We obtained sequences for three out of the four DNA markers which we had tried to sequences. We did not get the ITS-2 sequences for the species as the reads were always of bad quality. Out of these three successfully sequenced markers 18S rRNA and 28S rRNA was represented by a single haplotype, whereas *COI* was represented by two haplotypes: The 18S rRNA sequence (GenBank: MT261913), 1017 bp long; The 28S rRNA sequence (GenBank: MT261904), 780 bp long; The *COI* haplotype 1 sequence (GenBank: MT260372), 658 bp long; *COI* haplotype 2 sequence

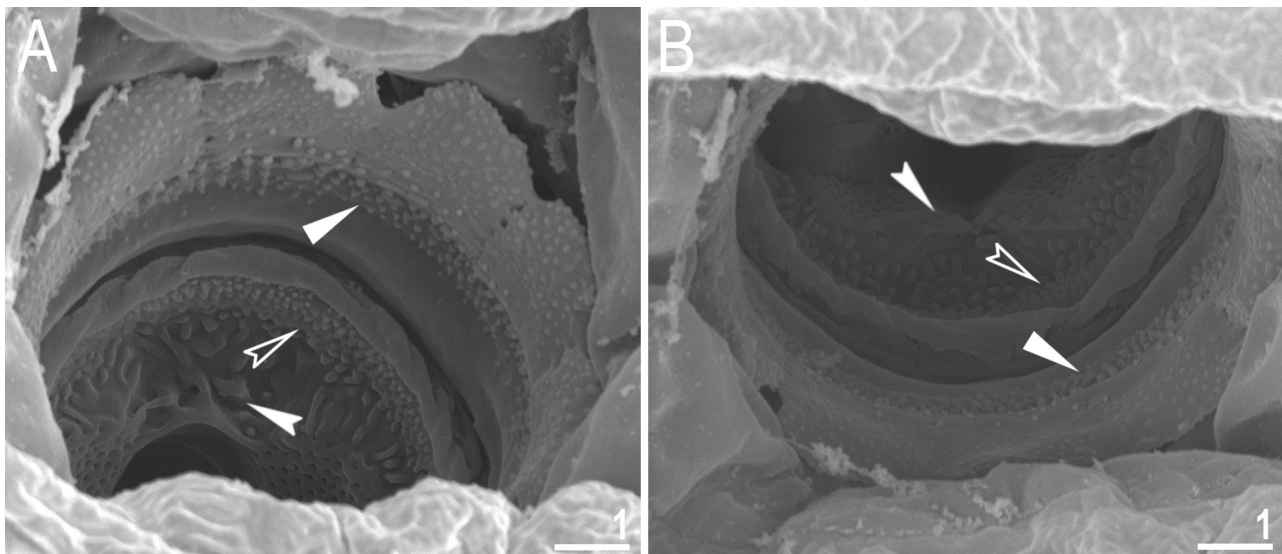


Fig. 5. *Macrobiotus crustulus* sp. nov., the oral cavity armature seen in SEM (paratypes). A–B, the oral cavity armature seen in SEM from different angles, dorsal (B) and ventral (C) view, respectively. Filled flat arrowheads indicate the first band of teeth in the oral cavity, empty indented arrowheads indicate the second band of teeth in the oral cavity, whereas filled indented arrowheads indicate the third band of teeth reduced to wrinkles and thickenings posterior to the second band of teeth. Scale bars in μm .

Table 5. Measurements [in μm] of selected morphological structures of the eggs of *Macrobiotus crustulus* sp. nov. eggs mounted in Hoyer’s medium

| Character | N | Range | Mean | SD |
|----------------------------------------------|----|------------|-------|-----|
| Egg bare diameter | 30 | 77.2–112.5 | 96.3 | 7.1 |
| Egg full diameter | 30 | 91.0–129.5 | 111.6 | 8.1 |
| Process height | 90 | 7.0–11.6 | 8.9 | 0.9 |
| Process base width | 90 | 5.7–10.5 | 8.1 | 0.9 |
| Process base/height ratio | 90 | 61%–109% | 91% | 11% |
| Terminal disc width | 90 | 5.3–9.8 | 7.5 | 0.8 |
| Inter-process distance | 90 | 2.1–5.8 | 3.8 | 0.7 |
| Number of processes on the egg circumference | 30 | 26–34 | 29.7 | 2.8 |

N, number of eggs/structures measured; Range, refers to the smallest and the largest structure among all measured specimens; SD, standard deviation.

(GenBank: MT260373), 658 bp long.

Remarks: *Paramacrobiotus filipi* sp. nov. is only the fourth species reported from Malaysia and the fourth

specifically from Borneo (Pilato et al. 2004; Gąsiorek 2018; Gąsiorek et al. 2020; Gąsiorek and Michalczyk 2020).

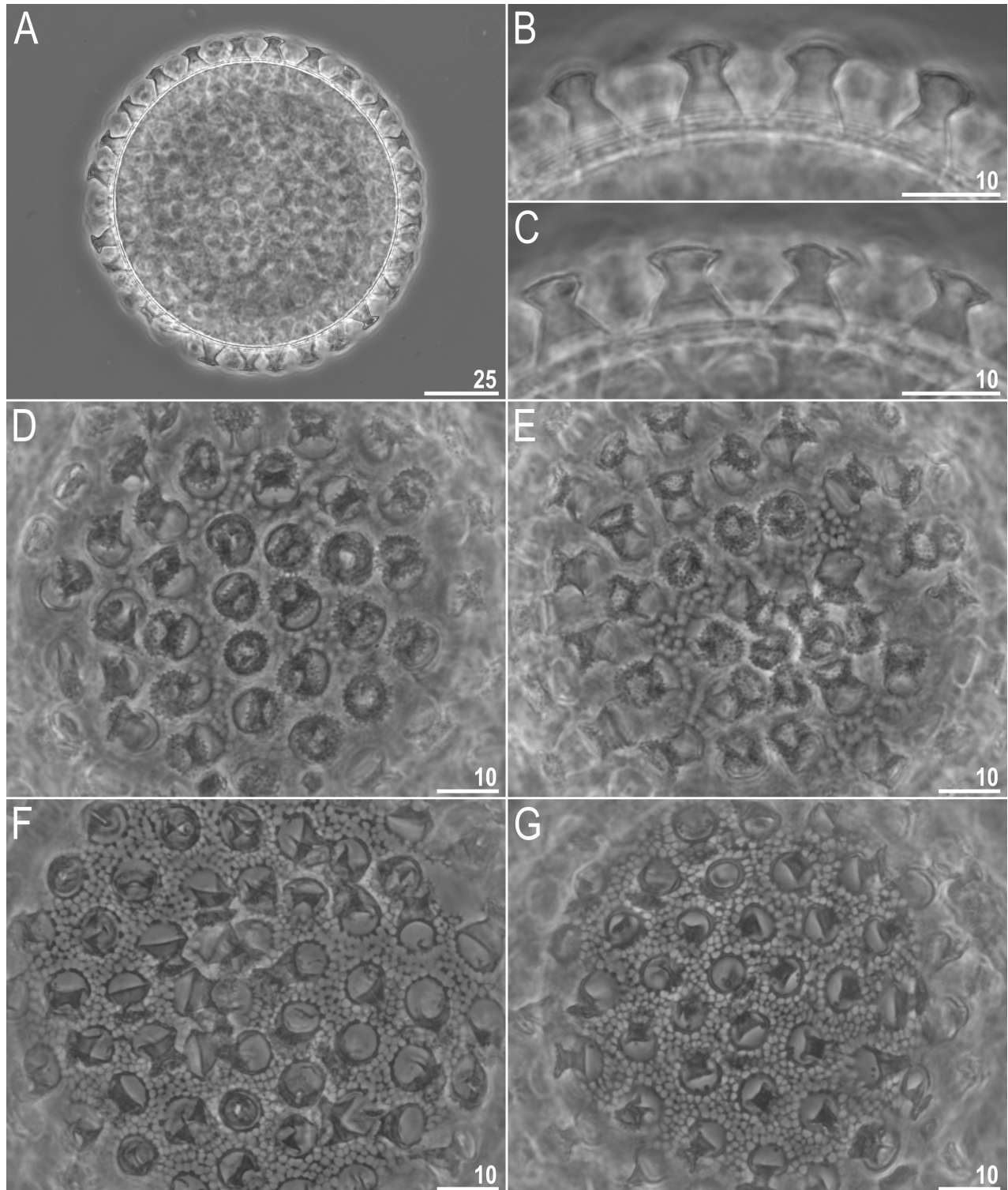


Fig. 6. *Macrobiotus crustulus* sp. nov., egg chorion morphology seen in PCM. A, midsection under 400× magnification; B–C, midsection under 1000× magnification; D–E, terminal discs under 1000× magnification; F–G, egg surface under 400× magnification. Scale bars in µm.

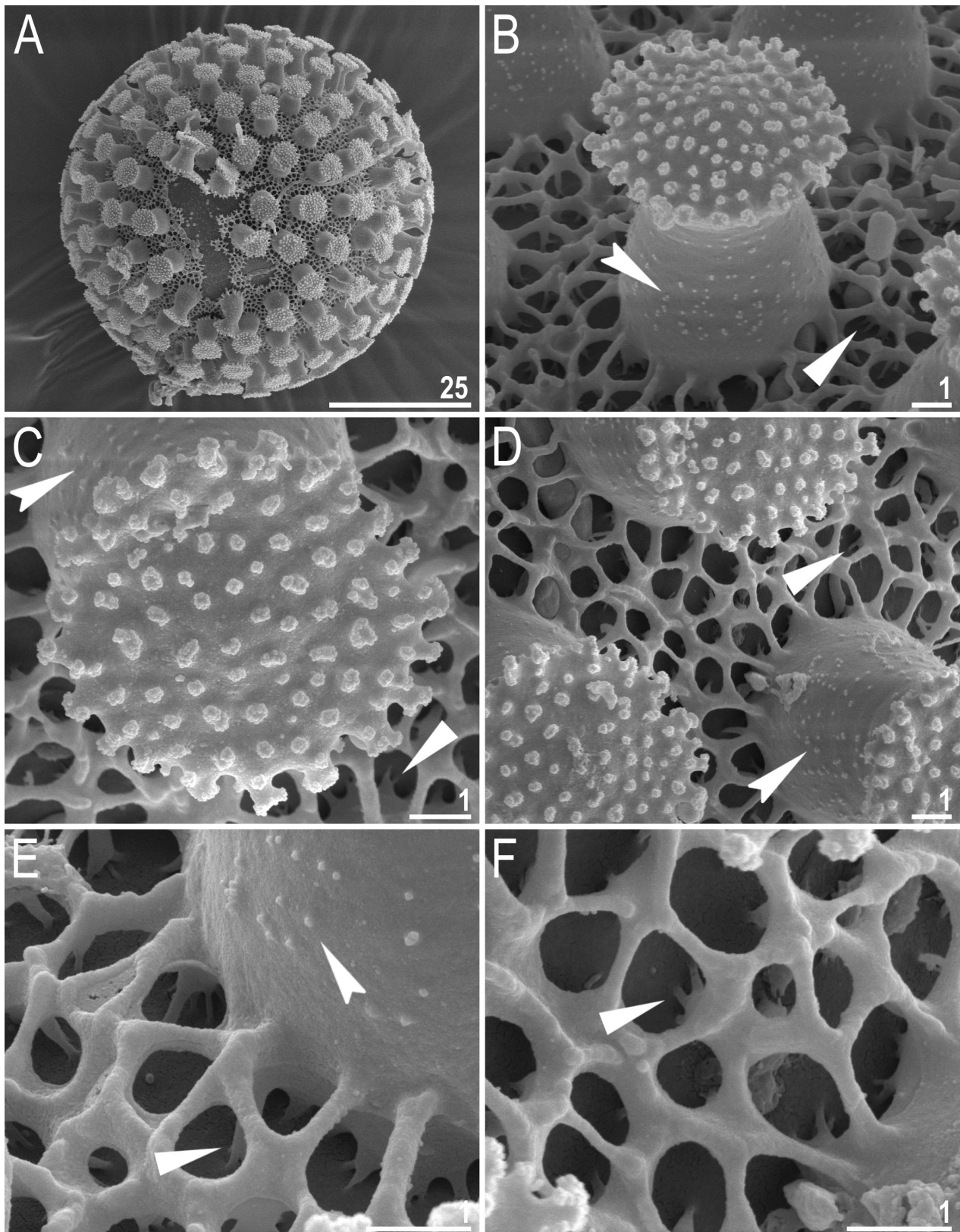


Fig. 7. *Macrobiotus crustulus* sp. nov., egg chorion morphology seen in SEM. A, entire egg; B, egg process; C–F, details of the egg processes and the reticulum. Filled indented arrowheads indicate granulation on process walls, filled flat arrowheads indicate fine connectors between the reticulum and egg surface. Scale bars in μm .

***Paramacrobotus alekseevi* (Tumanov, 2005)**

Material examined: Two slides (TH.001.01 and TH.001.02) with 1 paratype and 6 eggs from the type series mounted in Faure medium (these slides are now deposited at the Institute of Zoology and Biomedical Research, Jagiellonian University, Gronostajowa 9, 30-387, Kraków, Poland). PCM photomicrographs of the holotype and another paratype as well as two eggs from the type series.

Amended description of the species: According to the original description, the granulation is absent on the first three pairs of legs and lunules IV are faintly dentate. However, our re-examination of the type material revealed the presence of faint granulation present on the external surface of legs I–III in larger animals (Fig. 14A) whereas in smaller specimens the granulation can be hardly or even not visible. Moreover, we found that lunules on all the legs are smooth (Fig. 14A–B). The original description also states that indistinct reticular sculpture is present within the areolae. We confirmed

that the areolae surface is sculptured, however only wrinkles are present whereas reticulation or pores are absent or not visible under PCM (Fig. 14C–D). We also confirmed multiple divisions of the medio-ventral tooth in the third band of teeth into several roundish teeth (Fig. 14E–F) and the absence or invisibility of the body granulation under PCM.

DISCUSSION

Phenotypic differential diagnosis of *Macrobotus crustulus* sp. nov.

By having the *Macrobotus hufelandi* type of egg ornamentation (surface between processes covered with a reticulum) and convex terminal discs, the new species is the most similar to two other species of the *hufelandi* group: *Macrobotus martini* and *Macrobotus santoroi*. However, the new species can be easily distinguished from both species by having the *lissostomus* type of the

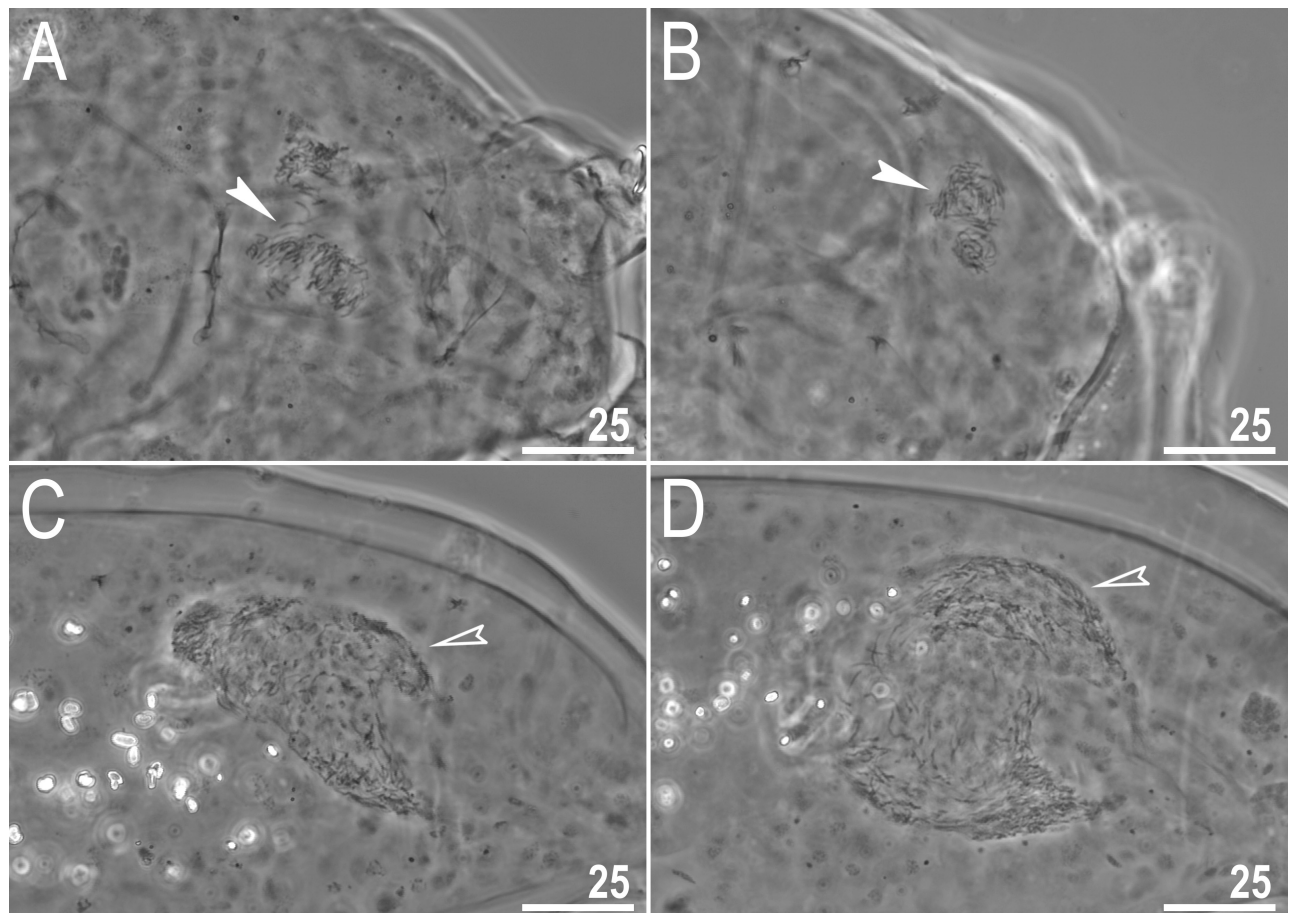


Fig. 8. *Macrobotus crustulus* sp. nov., reproduction (PCM, all paratypes). A–B, spermatheca visible in females freshly mounted in Hoyer’s medium with relaxed (A) and condensed (B) spermatozoa; C–D, testis visible in males freshly mounted in Hoyer’s medium. Filled indented arrowheads indicate spermatheca, empty indented arrowheads indicate testis. Scale bars in μm .

oral cavity armature where no teeth are visible under PCM, whereas *M. martini* and *M. santoroi* exhibit the *maculatus* and the *patagonicus* type of the oral cavity armature, respectively. Moreover, the new species differs specifically from:

M. martini, reported only from the USA (Great Smoky Mountains National Park) (Bartels et al. 2009; Nelson and Bartels 2013; Bertolani et al. 2014b), by: smaller cuticular pores (up to 2.4 μm in the new species vs 3.5 μm in *M. martini*), smooth lunules IV (lunules IV slightly dentate in *M. martini*), the presence of a subterminal constriction in the second macroplacoid (the second macroplacoid without constrictions in *M.*

martini), stylet supports inserted more anteriorly (*pt* = 69.3–72.7 in the new species vs *pt* = 72.9–74.9 in *M. martini*), a different morphology of the reticulation on the egg surface (peribasal meshes of similar size compared to interbasal meshes in the new species vs peribasal meshes distinctly larger compared to interbasal meshes in *M. martini*), a different morphology of terminal discs of egg processes (margins on the terminal discs slightly and densely indented with the disc surface covered by granulation vs. margins of terminal discs with poorly visible indentation and discs surface without granulation in *M. martini*), higher egg processes (7.0–11.6 μm in the new species vs 3.0–5.8 μm in *M.*

Table 6. Measurements [in μm] of selected morphological structures of individuals of *Paramacrobiotus filipi* sp. nov. individuals mounted in Hoyer’s medium

| Character | N | Range | | Mean | | SD | | Holotype | |
|--------------------------------|----|-----------|-----------|------|-----------|-----|-----------|----------|-----------|
| | | μm | <i>pt</i> | μm | <i>pt</i> | μm | <i>pt</i> | μm | <i>pt</i> |
| Body length | 20 | 245–537 | 778–1144 | 372 | 943 | 80 | 100 | 295 | 792 |
| Buccal tube | | | | | | | | | |
| Buccal tube length | 20 | 29.9–47.5 | – | 39.1 | – | 5.1 | – | 37.3 | – |
| Stylet support insertion point | 20 | 22.9–37.2 | 75.2–79.6 | 30.4 | 77.6 | 4.1 | 1.1 | 28.9 | 77.5 |
| Buccal tube external width | 20 | 5.2–10.4 | 16.7–22.4 | 7.7 | 19.4 | 1.6 | 1.8 | 8.0 | 21.4 |
| Buccal tube internal width | 20 | 3.9–7.9 | 12.9–17.5 | 6.0 | 15.1 | 1.2 | 1.4 | 5.9 | 15.8 |
| Ventral lamina length | 19 | 17.5–27.1 | 54.9–66.1 | 23.4 | 60.0 | 2.9 | 2.3 | 23.3 | 62.5 |
| Placoid lengths | | | | | | | | | |
| Macroplacoid 1 | 20 | 4.0–9.4 | 11.9–20.0 | 6.3 | 16.0 | 1.4 | 2.0 | 6.1 | 16.4 |
| Macroplacoid 2 | 20 | 2.4–6.2 | 8.0–13.8 | 4.3 | 10.9 | 1.1 | 1.6 | 3.7 | 9.9 |
| Macroplacoid 3 | 20 | 4.5–10.2 | 14.6–21.5 | 7.0 | 17.8 | 1.7 | 2.0 | 6.6 | 17.7 |
| Microplacoid | 20 | 1.5–3.5 | 4.0–8.6 | 2.5 | 6.3 | 0.5 | 1.1 | 1.9 | 5.1 |
| Macroplacoid row | 20 | 13.6–27.5 | 44.4–58.6 | 19.8 | 50.1 | 4.1 | 4.3 | 18.9 | 50.7 |
| Placoid row | 20 | 17.4–34.5 | 52.9–73.6 | 25.4 | 64.3 | 5.2 | 5.5 | 24.3 | 65.1 |
| Claw 1 heights | | | | | | | | | |
| External primary branch | 16 | 8.7–12.1 | 23.6–31.6 | 10.6 | 26.3 | 1.0 | 2.1 | 11.8 | 31.6 |
| External secondary branch | 16 | 6.2–9.1 | 14.9–23.6 | 8.0 | 19.8 | 0.8 | 2.1 | 8.8 | 23.6 |
| Internal primary branch | 15 | 8.8–12.2 | 21.8–29.5 | 10.0 | 25.4 | 1.0 | 2.0 | 9.2 | 24.7 |
| Internal secondary branch | 15 | 6.0–10.0 | 15.0–22.5 | 7.4 | 18.7 | 1.0 | 2.1 | 7.4 | 19.8 |
| Claw 2 heights | | | | | | | | | |
| External primary branch | 19 | 8.2–13.4 | 22.2–30.6 | 10.7 | 27.4 | 1.3 | 1.9 | 10.8 | 29.0 |
| External secondary branch | 20 | 6.2–10.2 | 15.9–23.7 | 8.2 | 21.0 | 1.1 | 1.9 | 8.0 | 21.4 |
| Internal primary branch | 19 | 6.9–11.9 | 23.1–27.7 | 9.7 | 25.0 | 1.3 | 1.5 | 9.0 | 24.1 |
| Internal secondary branch | 18 | 5.1–9.3 | 17.1–22.2 | 7.5 | 19.2 | 1.1 | 1.4 | ? | ? |
| Claw 3 heights | | | | | | | | | |
| External primary branch | 17 | 7.7–13.2 | 25.1–31.6 | 10.9 | 27.7 | 1.6 | 1.8 | 11.8 | 31.6 |
| External secondary branch | 18 | 5.7–10.4 | 17.3–23.7 | 8.3 | 21.1 | 1.3 | 1.6 | 8.6 | 23.1 |
| Internal primary branch | 17 | 7.4–12.3 | 22.8–28.5 | 10.0 | 25.8 | 1.5 | 1.6 | ? | ? |
| Internal secondary branch | 17 | 5.2–10.4 | 15.2–24.0 | 7.7 | 19.6 | 1.5 | 2.1 | ? | ? |
| Claw 4 heights | | | | | | | | | |
| Anterior primary branch | 11 | 8.1–13.9 | 27.1–36.2 | 11.2 | 30.4 | 1.9 | 3.1 | 13.3 | 35.7 |
| Anterior secondary branch | 13 | 4.9–13.5 | 16.4–29.2 | 8.8 | 21.7 | 2.1 | 3.5 | 10.4 | 27.9 |
| Posterior primary branch | 5 | 10.3–15.0 | 30.1–32.0 | 12.4 | 31.2 | 1.9 | 0.7 | 11.6 | 31.1 |
| Posterior secondary branch | 7 | 6.0–10.5 | 18.9–23.9 | 8.9 | 21.7 | 1.6 | 2.0 | 8.9 | 23.9 |

N, number of specimens/structures measured; Ranger, refers to the smallest and the largest structure among all measured specimens; SD, standard deviation).

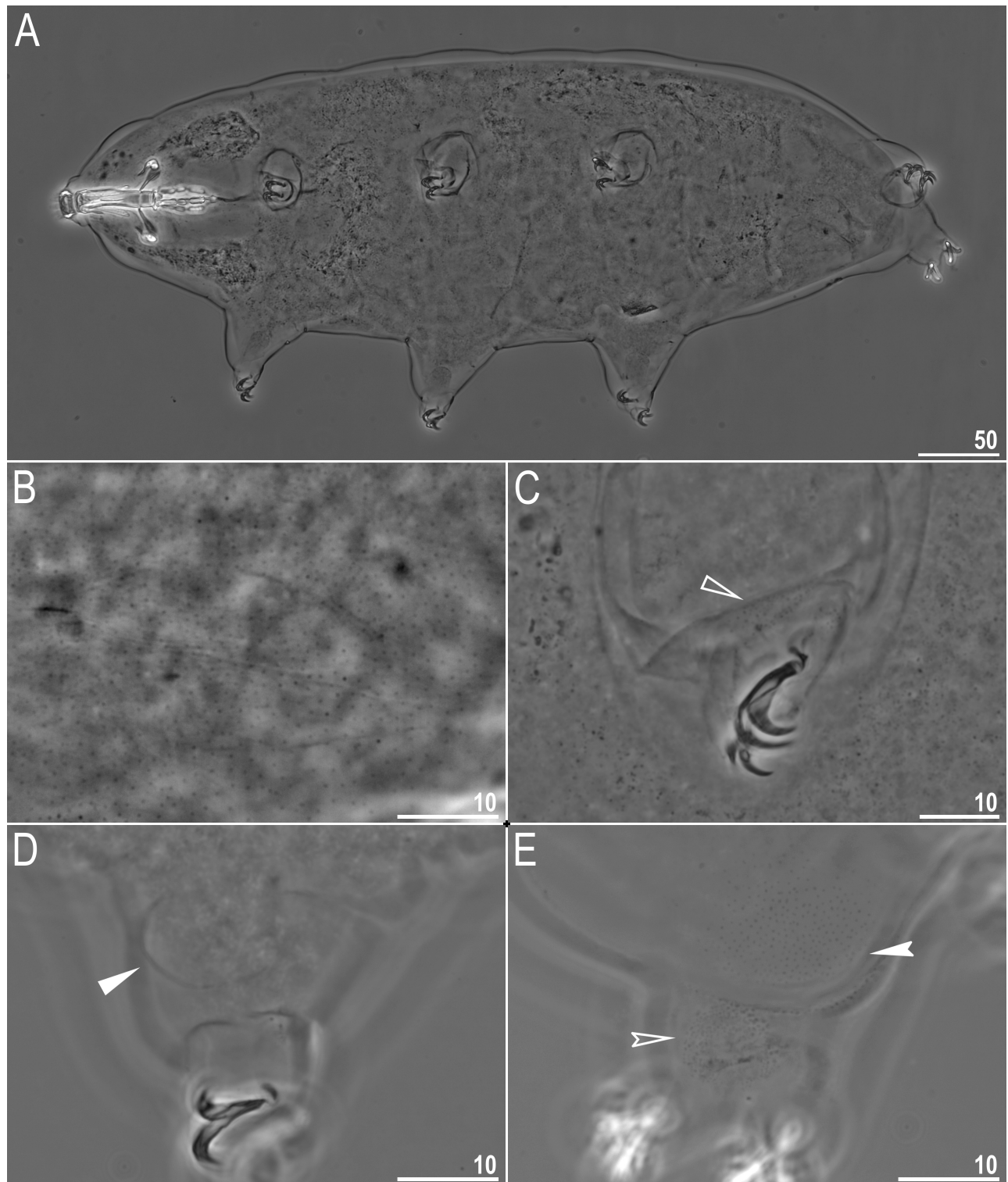


Fig. 9. *Paramacrobiotus filipi* sp. nov., habitus, body granulation and cuticular structures on legs (PCM). A, dorso-ventral projection (holotype, Hoyer's medium); B, body granulation on the dorso-caudal part of the body (paratype); C, granulation on the external surface of leg II (paratype); D, pulvinus on the internal surface of leg II (paratype); E, granulation on leg IV (holotype). Empty flat arrowhead indicates granulation on the external leg surface, filled flat arrowhead indicates a pulvinus, filled and empty indented arrowheads indicate les and more denser granulation on leg IV, respectively. Scale bars in μm.

martini), and by wider terminal discs of egg processes (5.3–9.8 μm in the new species vs 2.5–5.0 μm in *M. martini*).

M. santoroi, reported only from its type locality in Australia (Pilato and D'Urso 1976), by: the presence of a subterminal constriction in the second macroplacoid (the second macroplacoid without constriction in *M. santoroi*), typically developed terminal discs of egg processes (processes peg-shaped, with strongly reduced terminal discs in *M. santoroi*), the presence of evident reticulation on the egg surface between the processes, with large meshes with a diameter that is always larger than the mesh walls and nodes (very fine mesh with evident and wide walls and nodes, giving the false impression of a granulated surface in *M. santoroi*), larger eggs (egg full and bare diameter respectively 91.0–129.5 μm and 77.2–112.5 μm in the new species vs up to 84.0 μm and up to 76.0 μm in *M. santoroi*), higher egg processes (7.0–11.6 μm in the new species vs up to 4.0 μm in *M. santoroi*), and by a lower number of

processes on the egg circumference (26–34 processes in the new species vs. 37–40 processes in *M. santoroi*).

Genotypic differential diagnosis of *Macrobotus crustulus* sp. nov.

The ranges of uncorrected genetic *p*-distances between the new species and species of the *Macrobotus hufelandi* complex, the sequences of which are available from GenBank, are as follows (from the most to the least conservative):

18S rRNA: 1.46–4.65% (2.82% on average), with the most similar being an undetermined *M. hufelandi* complex species from Spain (FJ435738–9), *Macrobotus canarius* Stec, Krzywański and Michalczyk, 2018 from Spain (MH063925), *Macrobotus macrocalix* Bertolani and Rebecchi, 1993 from Poland (MH063926) and the least similar being *Macrobotus polypiformis* Roszkowska, Ostrowska, Stec, Janko and Kaczmarek, 2017 from Ecuador (KX810008).

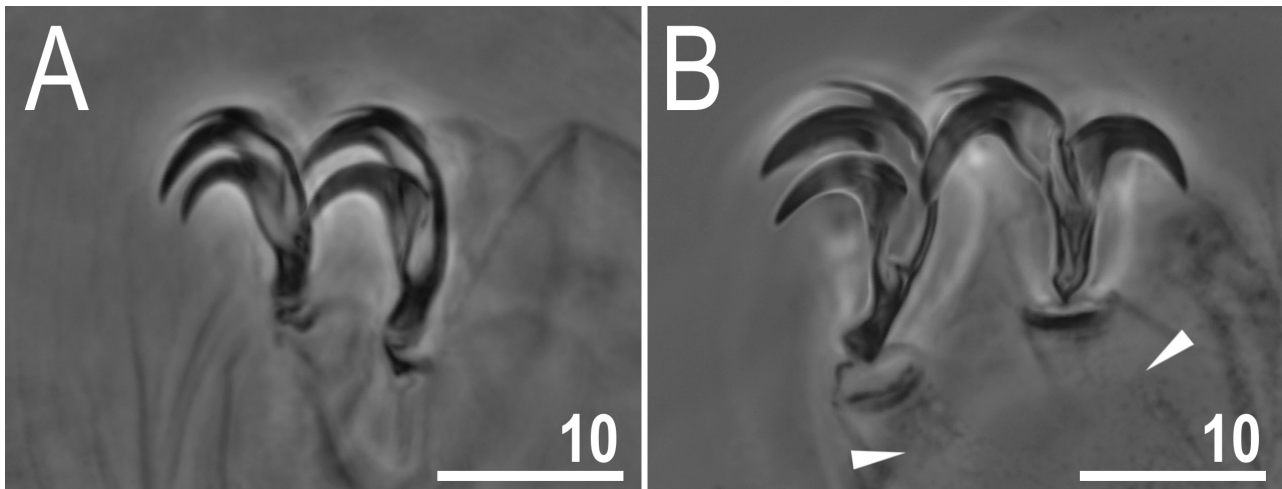


Fig. 10. *Paramacrobotus filipi* sp. nov., claws (PCM). A–B, claws II (A, paratype) and IV (B, holotype). Filled flat arrowheads arrowhead indicate the horseshoe structure connecting the anterior and the posterior claw. Scale bars in μm.

Table 7. Measurements [in μm] of selected morphological structures of the eggs of *Paramacrobotus filipi* sp. nov. mounted in Hoyer’s medium

| Character | N | Range | Mean | SD |
|----------------------------------------------|----|------------|-------|-----|
| Egg bare diameter | 5 | 61.4–65.4 | 63.9 | 1.7 |
| Egg full diameter | 5 | 99.0–104.5 | 102.4 | 2.4 |
| Process height | 29 | 17.8–25.2 | 20.7 | 1.8 |
| Process base width | 29 | 11.7–21.7 | 16.5 | 2.4 |
| Process base/height ratio | 29 | 55%–100% | 80% | 12% |
| Inter-process distance | 26 | 2.0–7.1 | 4.7 | 1.4 |
| Number of processes on the egg circumference | 4 | 10–11 | 10.3 | 0.5 |

N, number of eggs/structures measured; Range, refers to the smallest and the largest structure among all measured specimens; SD, standard deviation.

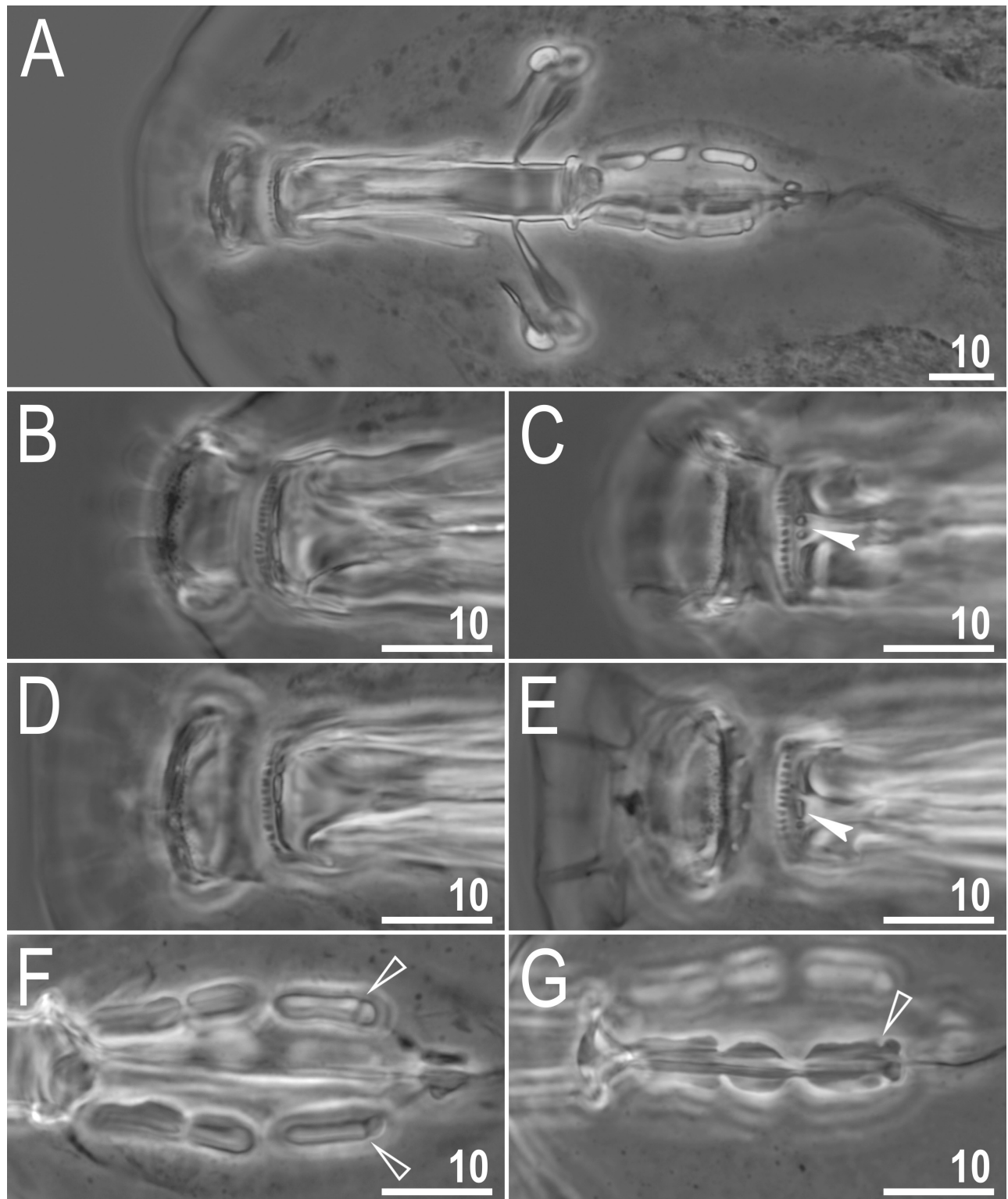


Fig. 11. *Paramacrobiotus filipi* sp. nov., buccal apparatus and the oral cavity armature seen in PCM. A, dorso-ventral projection of the buccal apparatus (paratype); B–D, oral cavity armature, dorsal (B, D) and ventral (C, E) view (B and C holotype, D and E paratype); F–G, placoid morphology, dorsal (F, holotype) and ventral (E, paratype) view. Filled indented arrowheads indicate the subdivided medio-ventral tooth of the third band of teeth, flat empty arrowheads indicate the subterminal constriction in the third macroplacoid. Scale bars in μm .

28S rRNA: 6.22–12.89% (8.86% on average), with the most similar being *M. macrocalix* from Poland (MH063935) and the least similar being *M. polypiformis* from Ecuador (KX810009).

ITS-2: 15.15–30.81% (21.04% on average), with the most similar being *M. canaricus* from Spain (MH063928) and the least similar *M. scoticus* Stec, Morek, Gąsiorek, Blagden and Michalczyk, 2017 from Scotland (KY797268).

COI: 20.13–26.79% (22.23% on average), with the most similar being *M. terminalis* Bertolani and Rebecchi, 1993 from Italy (AY598775) and the least similar being *M. papei* Stec, Kristensen and Michalczyk, 2018 from Tanzania (MH057763).

Phenotypic differential diagnosis of *P. filipi* sp. nov.

By having three macroplacoids and a microplacoid, granulation on all legs, all lunules smooth and eggs with processes terminated with small terminal discs, the new species is very similar to *P. alekseevi*, reported only from its type locality in Thailand (Tumanov 2005) and from China (Beasley and Miller 2007), but differs from it specifically by: the presence of body granulation which is visible under PCM (granulation absent or not visible under PCM in *P. alekseevi*), the medio-ventral tooth subdivided into two smaller teeth (medio-ventral tooth always subdivided

into three to five smaller teeth in *P. alekseevi*), and by porous areoles (areoles without pores or pores not visible under PCM in *P. alekseevi*).

Genotypic differential diagnosis of *P. filipi* sp. nov.

The ranges of uncorrected genetic *p*-distances between the new species and species of the genus *Paramacrobiotus*, for which sequences are available from GenBank, are as follows (from the most to the least conservative):

18S rRNA: 1.86–4.53% (2.18% on average), with the most similar being *P. richtersi* s.s. (Murray, 1911) from Ireland (MK041023), *P. spatialis* Guidetti, Cesari, Bertolani, Altiero and Rebecchi, 2019 from Italy (MK041024–6), *P. fairbanksi* Schill, Forster, Dandekar and Wolf, 2010 from Italy and Poland (MK041027–9, MH664941–2), *P. depressus* Guidetti, Cesari, Bertolani, Altiero and Rebecchi, 2019 from Italy (MK041030), *P. celsus* Guidetti, Cesari, Bertolani, Altiero and Rebecchi, 2019 from Italy (MK041031), *P. arduus* Guidetti, Cesari, Bertolani, Altiero and Rebecchi, 2019 from Italy (MK041032), an undetermined *P. richtersi* complex species from Italy, Portugal, New Zealand, Norway, France and Australia (HQ604985–6, MH664932, MH664934, MH664939–42, MH664944) and the least similar being *P. areolatus* (Murray, 1907) from Norway (MH664931).

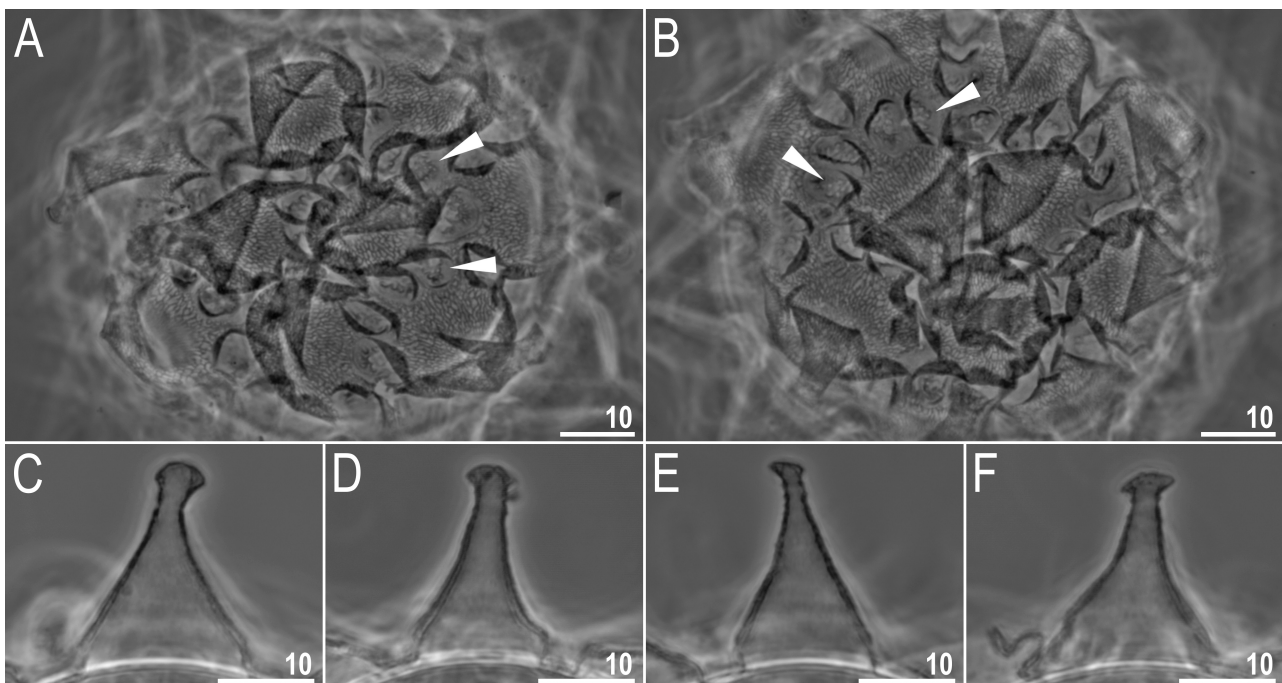


Fig. 12. *Paramacrobiotus filipi* sp. nov., egg chorion morphology seen in PCM. A–B, egg surface under 1000× magnification; C–F, midsections of egg processes under 1000× magnification. Filled flat arrowheads indicate sculptured and porous areole surface. Scale bars in μm .

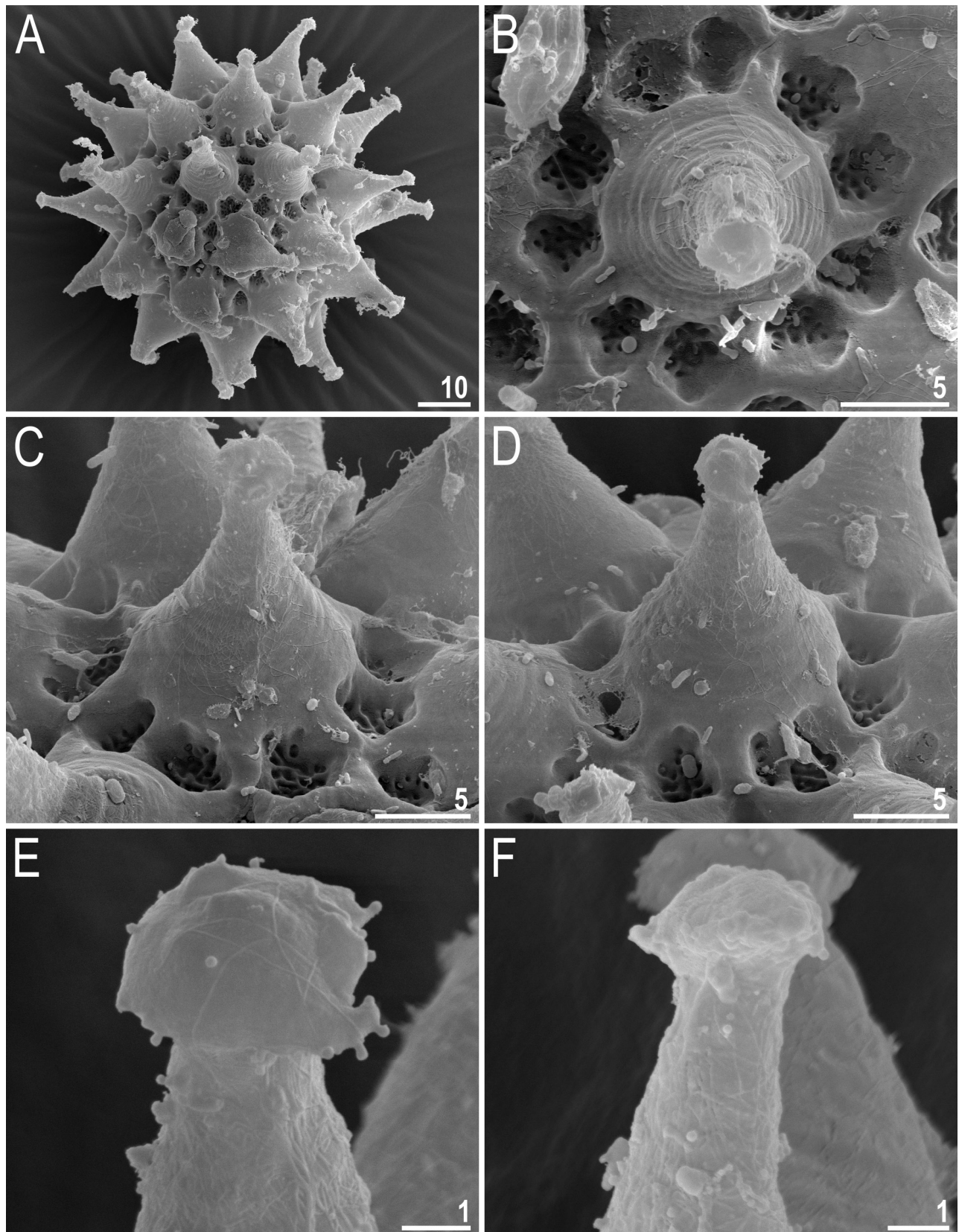


Fig. 13. *Paramacrobiotus filipi* sp. nov., egg chorion morphology seen in SEM. A, entire egg; B–D, magnification on the egg processes and areoles; E–F, details of the egg processes apices terminated small terminal discs. Scale bars in μm.

28S rRNA: 3.63–8.65% (5.06% on average), with the most similar being *P. experimentalis* Kaczmarek, Mioduchowska, Poprawa and Roszkowska, 2020 from Madagascar (MN073466–5) and the least similar being *P. areolatus* from Norway (MH664948).

COI: 22.16–27.05% (24.51% on average), with the most similar being an undetermined *P. richtersi* complex species from Brazil (MH676002) and the least similar being *P. arduus* from Italy (MK041022).

CONCLUSIONS

We identified two new tardigrade species using an integrative approach based on morphological distinctions to congeners and a genetic comparison using four DNA fragments. Moreover, *Macrobotus crustulus* sp. nov. is the first ever tardigrade species reported from French Guiana, whereas *Paramacrobotus filipi* sp. nov. is only the fourth species reported from Malaysia.

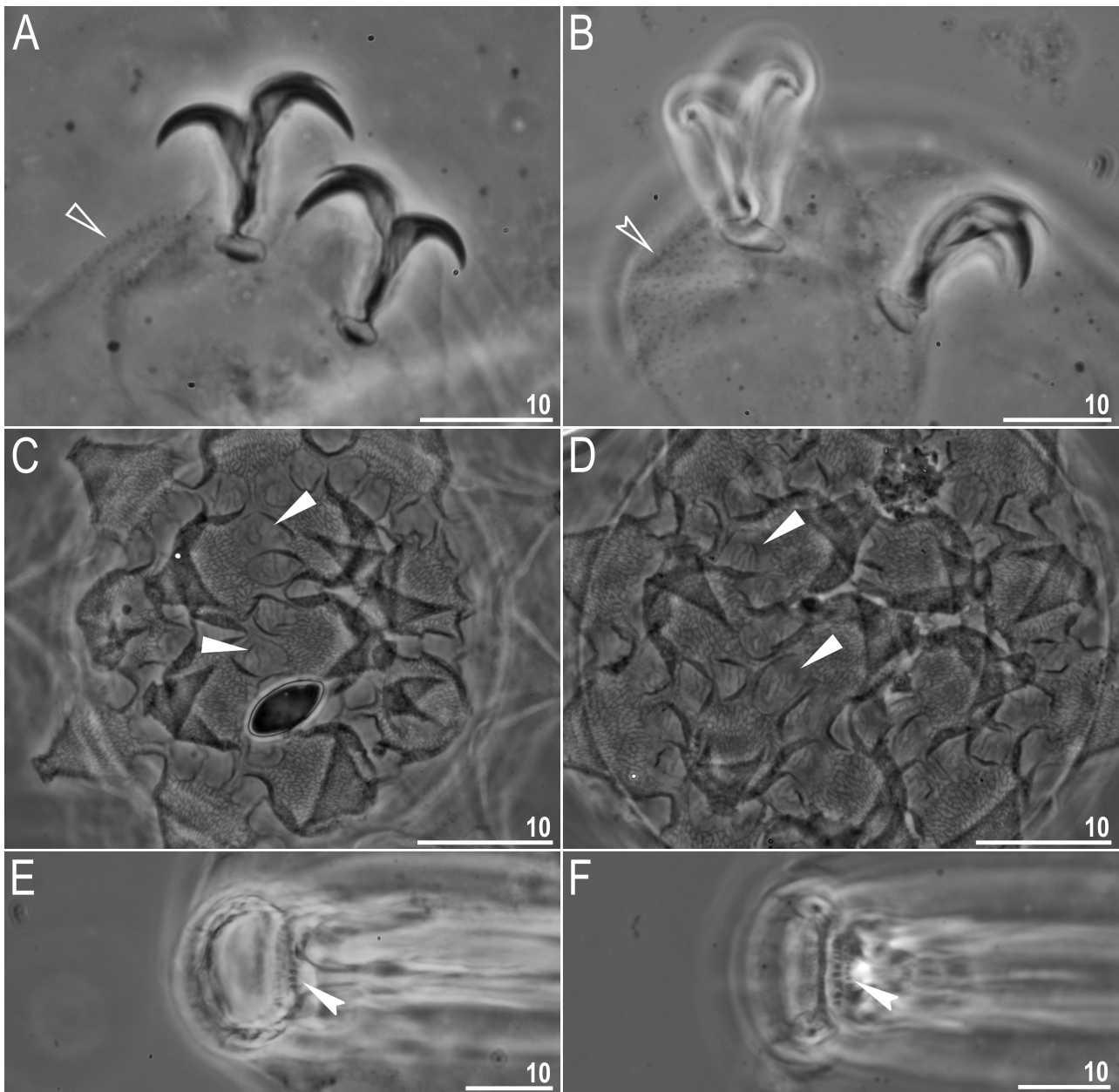


Fig. 14. *Paramacrobotus alekseevi* (Tumanov, 2005), details of animals and egg chorion morphology (PCM). A–B, granulation and claws on legs III (A, holotype) and IV (B, holotype); C–D, egg surface under 1000 \times magnification; E–F, ventral view on the oral cavity armature (E – holotype, F – paratype). Empty flat and indented arrowheads indicate granulation on leg III and IV, respectively, filled flat arrowheads indicate sculptures areoles without pores, filled indented arrowheads indicate subdivided medio-ventral tooth of the third band of teeth. Scale bars in μm .

Moreover, the re-examination of the type material of *P. alekseevi* enabled us to amend its description.

Acknowledgment: This work and the new species name have been registered with ZooBank under urn:lsid:zoobank.org:pub:C81767B5-2BA3-402A-93C1-1DFBAD256482. We would like to thank to our colleagues Bartłomiej Surmacz, Witold Morek and Piotr Gąsiorek for collecting the samples which allowed us to conduct this study. The sampling in Borneo was supported by the Polish Ministry of Science and Higher Education via the Diamond Grant (DI2015 014945 to Piotr Gąsiorek, supervised by Łukasz Michalczyk). We are also very grateful Denis Tumanov for sending us the type material and microphotographs of type specimens of *P. alekseevi* and to Witold Morek for his help with SEM imaging. Finally we are also indebted to two anonymous reviewers for their valuable comments and suggestion on our manuscript. The study was supported by the *Sonata Bis* programme of the Polish National Science Centre (grant no. 2016/22/E/NZ8/00417 to ŁM) and by the grant from the European Commission's programme "Transnational Access to Major Research Infrastructures" to SYNTHESYS (grant no. DK-TAF-2693 to DS).

Authors' contributions: DS and ŁM conceived the study. DM collected and analysed molecular data. DS and MD examined the sample, provided the measurements and photographs of the new species, prepared the figures and drafted the manuscript. ŁM supervised the entire process and drafted the manuscript. All the authors read and approved the final manuscript.

Competing interests: The authors declare that they have no competing interests.

Availability of data and materials: The slides and SEM stubs are deposited at the Institute of Zoology and Biomedical Research, Jagiellonian University, Gronostajowa 9, 30-387 Kraków, Poland.

Consent for publication: Not applicable.

Ethics approval consent to participate: Not applicable.

REFERENCES

- Bartels P, Pilato G, Lisi O, Nelson DR. 2009. *Macrobiotus* (Eutardigrada, Macrobiotidae) from the Great Smoky Mountains National Park, Tennessee/North Carolina, USA (North America): two new species and six new records. *Zootaxa* **2022**:45–57. doi:10.11646/zootaxa.2022.1.4.
- Beasley CW, Miller WR. 2007. Tardigrada of Xinjiang Uygur Autonomous Region, China. *J Limnol* **66**:49–55. doi:10.4081/jlimnol.2007.s1.49.
- Bertolani R, Bartels PJ, Guidetti R, Cesari M, Nelson DR. 2014b. Aquatic tardigrades in the Great Smoky Mountains National Park, North Carolina and Tennessee, U.S.A., with the description of a new species of *Thulinus* (Tardigrada, Isohypsibiidae). *Zootaxa* **3764**(5):524–536. doi:10.11646/zootaxa.3764.5.2.
- Bertolani R, Biserov V, Rebecchi L, Cesari M. 2011b. Taxonomy and biogeography of tardigrades using an integrated approach: new results on species of the *Macrobiotus hufelandi* group. *Invertebrate Zoology* **8**(1):23–36. doi:10.15298/invertzool.08.1.05.
- Bertolani R, Guidetti R, Marchioro T, Altiero T, Rebecchi L, Cesari M. 2014a. Phylogeny of Eutardigrada: New molecular data and their morphological support lead to the identification of new evolutionary lineages. *Mol Phylogenet Evol* **76**:110–126. doi:10.1016/j.ympev.2014.03.006.
- Bertolani R, Rebecchi L. 1993. A revision of the *Macrobiotus hufelandi* group (Tardigrada, Macrobiotidae), with some observations on the taxonomic characters of eutardigrades. *Zool Scr* **22**:127–152. doi:10.1111/j.1463-6409.1993.tb00347.x.
- Bertolani R, Rebecchi L, Giovannini I, Cesari M. 2011a. DNA barcoding and integrative taxonomy of *Macrobiotus hufelandi* C.A.S. Schultz 1834, the first tardigrade species to be described, and some related species. *Zootaxa* **2997**:19–36. doi:10.11646/zootaxa.2997.1.2.
- Binda MG, Pilato G. 1984. *Macrobiotus sapiens*, nuova specie di Eutardigrada di Sicilia. *Animalia* **11**:85–90.
- Bochnak M, Vončina K, Kristensen RM, Gąsiorek P. 2020. Continued exploration of Tanzanian rainforests reveals a new echiniscid species (Heterotardigrada). *Zool Stud* **59**:18. doi:10.6620/ZS.2020.59-18.
- Caicedo M, Arquez M, Castro LR, Quiroga S. 2017. Genetic barcoding in a *Paramacrobiotus* species (Tardigrada: Parachela) in Santa Mata, Colombia. *Revista Intropica* **12**:1. doi:10.21676/23897864.2125.
- Casquet JT, Thebaud C, Gillespie RG. 2012. Chelex without boiling, a rapid and easy technique to obtain stable amplifiable DNA from small amounts of ethanol-stored spiders. *Mol Ecol Resour* **12**:136–141. doi:10.1111/j.1755-0998.2011.03073.x.
- Cesari M, Bertolani R, Rebecchi L, Guidetti R. 2009. DNA barcoding in Tardigrada: the first case study on *Macrobiotus macrocalix* Bertolani & Rebecchi 1993 (Eutardigrada, Macrobiotidae). *Mol Ecol Resour* **9**(3):699–706. doi:10.1111/j.1755-0998.2009.02538.x.
- Cesari M, Giovanni I, Bertolani R, Rebecchi L. 2011. An example of problems associated with DNA barcoding in tardigrades: a novel method for obtaining voucher specimens. *Zootaxa* **3104**:42–51. doi:10.11646/zootaxa.3104.1.3.
- Coughlan K, Michalczyk Ł, Stec D. 2019. *Macrobiotus caelestis* sp. nov., a new tardigrade species (Macrobiotidae: *hufelandi* group) from the Tien Shan Mountains (Kyrgyzstan). *Annales Zoologici* **69**(3):499–513. doi:10.3161/00034541ANZ2019.69.3.002.
- Coughlan K, Stec D. 2019. Two new species of the *Macrobiotus hufelandi* complex (Tardigrada: Eutardigrada: Macrobiotidae) from Australia and India, with notes on their phylogenetic position. *Eur J Taxon* **573**:1–38. doi:10.5852/ejt.2019.573.
- Dasty H. 1980. Niesporczaki (Tardigrada) Tatrzańskiego Parku Narodowego. *Monografie Fauny Polski* **9**:1–232.
- Degma P, Bertolani R, Guidetti R. 2009–2019. Actual checklist of Tardigrada species. doi:10.25431/11380_1178608.
- Degma P, Guidetti R. 2007. Notes to the current checklist of Tardigrada. *Zootaxa* **1579**:41–53. doi:10.11646/zootaxa.1579.1.2.

- Doyère LMF. 1840. Memoire sur les Tardigrades. I. Ann Sci Nat Paris Series 2 **14**:269–362.
- Folmer O, Black M, Hoeh W, Lutz R, Vrijenhoek R. 1994. DNA primers for amplification of mitochondrial cytochrome c oxidase subunit I from diverse metazoan invertebrates. Mol Mar Biol Biotechnol **3**:294–299.
- Gąsiorek P, Michalczyk Ł. 2020. Phylogeny of Itaquasconinae in light of the evolution of the flexible pharyngeal tube in Tardigrada. Zool Scr **49**:499–511. doi:10.1111/zsc.12424.
- Gąsiorek P, Stec D, Zawierucha Z, Kristensen RM, Michalczyk Ł. 2018. Revision of *Testechiniscus* Kristensen, 1987 (Heterotardigrada: Echiniscidae) refutes the polar-temperate distribution of the genus. Zootaxa **4472**(2):261–297. doi:10.11646/zootaxa.4472.2.3.
- Gąsiorek P, Vončina K, Michalczyk Ł. 2020. An overview of the sexual dimorphism in *Echiniscus* (Heterotardigrada, Echiniscoidea), with the description of *Echiniscus masculinus* sp. nov. (the *virginicus* complex) from Borneo. Zoosyst Evol **96**(1):103–113. doi:10.3897/zse.96.49989.
- Gąsiorek P. 2018. New *Bryodelphax* species (Heterotardigrada: Echiniscidae) from Western Borneo (Sarawak), with new molecular data for the genus. Raffles B Zool **66**:371–381.
- Guidetti R, Bertolani R. 2005. Tardigrade taxonomy: an updated check list of the taxa and a list of characters for their identification. Zootaxa **845**:1–46. doi:10.11646/zootaxa.845.1.1.
- Giribet G, Carranza S, Baguña J, Riutort M, Ribera C. 1996. First molecular evidence for the existence of a Tardigrada + Arthropoda clade. Mol Biol Evol **13**:76–84. doi:10.1093/oxfordjournals.molbev.a025573.
- Guidetti R, Cesari M, Bertolani R, Altiero T, Rebecchi L. 2019. High diversity in species, reproductive modes and distribution within the *Paramacrobrotus richtersi* complex (Eutardigrada, Macrobiotidae). Zool Lett **5**:1. doi:10.1186/s40851-018-0113-z.
- Guidetti R, Gandolfi A, Rossi V, Bertolani R. 2005. Phylogenetic analysis of Macrobiotidae (Eutardigrada, Parachela): a combined morphological and molecular approach. Zool Scr **34**:235–244. doi:10.1111/j.1463-6409.2005.00193.x.
- Guidetti R, Peluffo JR, Rocha AM, Cesari M, Moly de Peluffo MC. 2013. The morphological and molecular analyses of a new South American urban tardigrade offer new insights on the biological meaning of the *Macrobrotus hufelandi* group of species (Tardigrada: Macrobiotidae). J Nat Hist **47**(37–38):2409–2426. doi:10.1080/00222933.2013.800610.
- Guidetti R, Schill RO, Bertolani R, Dandekar T, Wolf M. 2009. New molecular data for tardigrade phylogeny, with the erection of *Paramacrobrotus* gen. nov. J Zool Syst Evol Res **47**(4):315–321. doi:10.1111/j.1439-0469.2009.00526.x.
- Guil N, Giribet G. 2012. A comprehensive molecular phylogeny of tardigrades – adding genes and taxa to a poorly resolved phylum-level phylogeny. Cladistics **28**(1):21–49. doi:10.1111/j.1096-0031.2011.00364.x.
- Hall TA. 1999. BioEdit: a user-friendly biological sequence alignment editor and analysis program for Windows 95/98/NT. Nucleic Acids Symp Ser **41**:95–98.
- Kaczmarek Ł, Cytan J, Zawierucha K, Diduszko D, Michalczyk Ł. 2014. Tardigrades from Peru (South America), with descriptions of three new species of Parachela. Zootaxa **3790**:357–379. doi:10.11646/zootaxa.3790.2.5.
- Kaczmarek Ł, Gawlak M, Bartels PJ, Neslon DR, Roszkowska M. 2017. Revision of the genus *Paramacrobrotus* Guidetti et al., 2009 with the description of a new species, re-descriptions and a key. Annales Zoologici **67**(4):627–656. doi:10.3161/00034541ANZ2017.67.4.001.
- Kaczmarek Ł, Michalczyk Ł. 2017. The *Macrobrotus hufelandi* (Tardigrada) group revisited. Zootaxa **4363**:101–123. doi:10.11646/zootaxa.4363.1.4.
- Kaczmarek Ł, Roszkowska M, Poprawa I, Janelt K, Kmita H, Gawlak M, Fiałkowska E, Mioduchowska M. 2020. Integrative description of bisexual *Paramacrobrotus experimentalis* sp. nov. (Macrobiotidae) from republic of Madagascar (Africa) with microbiome analysis. Mol Phylogenet Evol **145**:106730. doi:10.1016/j.ympev.2019.106730.
- Katoh K, Misawa K, Kuma K, Miyata T. 2002. MAFFT: a novel method for rapid multiple sequence alignment based on fast Fourier transform. Nucleic Acids Res **30**:3059–66. doi:10.1093/nar/gkf436.
- Katoh K, Toh H. 2008. Recent developments in the MAFFT multiple sequence alignment program. Brief Bioinform **9**:286–298. doi:10.1093/bib/bbn013.
- Kayastha P, Berdi D, Mioduchowska M, Gawlak M, Łukasiewicz A, Goldyn B, Kaczmarek Ł. 2020. Some tardigrades from Nepal (Asia) with integrative description of *Macrobrotus wandae* sp. nov. (Macrobiotidae: *hufelandi* group). Annales Zoologici **70**:121–142. doi:10.3161/00034541ANZ2020.70.1.007.
- Kumar S, Stecher G, Tamura K. 2016. MEGA7: Molecular Evolutionary Genetics Analysis version 7.0 for bigger datasets. Mol Biol Evol **33**:1870–1874. doi:10.1093/molbev/msw054.
- Marley NJ, McInnes SJ, Sands CJ. 2011. Phylum Tardigrada: A re-evaluation of the Parachela. Zootaxa **2819**:51–64. doi:10.11646/zootaxa.2819.1.2.
- Michalczyk Ł, Kaczmarek Ł. 2003. A description of the new tardigrade *Macrobrotus reinhardti* (Eutardigrada, Macrobiotidae, *harmsworthi* group) with some remarks on the oral cavity armature within the genus *Macrobrotus* Schultz. Zootaxa **331**:1–24. doi:10.11646/zootaxa.331.1.1.
- Michalczyk Ł, Kaczmarek Ł. 2013. The Tardigrada Register: a comprehensive online data repository for tardigrade taxonomy. J Limnol **72**:175–181. doi:10.4081/jlimnol.2013.s1.e22.
- Mironov SV, Dabert J, Dabert M. 2012. A new feather mite species of the genus *Proctophyllodes* Robin, 1877 (Astigmata: Proctophyllodidae) from the Long-tailed Tit *Aegithalos caudatus* (Passeriformes: Aegithalidae): morphological description with DNA barcode data. Zootaxa **3253**:54–61. doi:10.11646/zootaxa.3253.1.2.
- Morek W, Stec D, Gąsiorek P, Schill RO, Kaczmarek Ł, Michalczyk Ł. 2016. An experimental test of eutardigrade preparation methods for light microscopy. Zool J Linnean Soc **178**:785–793. doi:10.1111/zoj.12457.
- Murray J. 1907. Arctic Tardigrada, collected by William S. Bruce. Earth Env Sci T R So **45**:669–681.
- Murray J. 1911. Clare Island Survey Arctiscoida. Proc R Ir Acad C **31**:1–16.
- Nelson DR, Bartels PJ. 2013. Species richness of soil and leaf litter tardigrades in the Great Smoky Mountains National Park (North Carolina/Tennessee, USA). J Limnol **72**:144–151. doi:10.4081/jlimnol.2013.s1.e18.
- Nelson DR, Guidetti R, Rebecchi L. 2015. Phylum Tardigrada. In: Thorp and Covich's Freshwater Invertebrates. Academic Press, pp. 347–380. doi:10.1016/B978-0-12-385026-3.00017-6.
- Nowak B, Stec D. 2018. An integrative description of *Macrobrotus hannaes* sp. nov. (Tardigrada: Eutardigrada: Macrobiotidae: *hufelandi* group) from Poland. Turk J Zool **42**:269–286. doi:10.3906/zoo-1712-31.
- Pilato G, Binda MG. 2010. Definition of families, subfamilies, genera and subgenera of the Eutardigrada, and keys to their identification. Zootaxa **2404**:1–52. doi:10.11646/zootaxa.2404.1.1.
- Pilato G, Binda MG, Lisi O. 2004. *Famelobrotus salici*, n. gen. n. sp.,

- a new eutardigrade from Borneo. *New Zeal J Zool* **31**:57–60. doi:10.1080/03014223.2004.9518359.
- Pilato G, Binda MG. 1983. Descrizione di una nuova specie di Eutardigrada d’Australia *Macrobiotus joannae* n. sp. *Animalia* **10**:262–272.
- Pilato G, D’Urso V. 1976. Contributo alla conoscenza dei Tardigradi d’Australia. *Animalia* **3**:135–145.
- Pilato G, Kaczmarek Ł, Michalczyk Ł, Lisi O. 2003. *Macrobiotus polonicus*, a new species of Tardigrada from Poland (Eutardigrada, Macrobiotidae, 'hufelandi group'). *Zootaxa* **258**:1–8. doi:10.11646/zootaxa.258.1.1.
- Pilato G. 1981. Analisi di nuovi caratteri nello studio degli Eutardigradi. *Animalia* **8**:51–57.
- Ramazotti G. 1956. Tre nuove specie di Tardigradi ed altre specie poco comuni. *Atti Soc Nat Milano* **95**:284–291.
- Richters F. 1926. Tardigrada. In: Kükenthal, W. & Krumbach, T. (Eds.) *Handbuch der Zoologie* Vol. 3. Walter de Gruyter & Co., Berlin & Leipzig, pp. 58–61.
- Roszkowska M, Ostrowska M, Stec D, Janko K, Kaczmarek Ł. 2017. *Macrobiotus polypiformis* sp. nov., a new tardigrade (Macrobiotidae; *hufelandi* group) from the Ecuadorian Pacific coast, with remarks on the claw abnormalities in eutardigrades. *Eur J Taxon* **327**:1–19. doi:10.5852/ejt.2017.327.
- Schill RO, Forster F, Dandekar T, Wolf N. 2010. Using compensatory base change analysis of internal transcribed spacer 2 secondary structures to identify three new species in *Paramacrobiotus* (Tardigrada). *Org Divers Evol* **10**(4):287–296. doi:10.1007/s13127-010-0025-z.
- Schultze CAS. 1834. *Macrobiotus Hufelandii* animal e crustaceorum classe novum, reviviscendi post diuturnam asphixiam et aridiatem potens, etc. 8, 1 tab. C. Curths, Berlin, 6 pp, I Table.
- Schuster RO, Nelson DR, Grigarick AA, Christenberry D. 1980. Systematic criteria of the Eutardigrada. *T Am Microsc Soc* **99**:284–303.
- Stec D, Arakawa K, Michalczyk Ł. 2018d. An integrative description of *Macrobiotus shonanicus* sp. nov. (Tardigrada: Macrobiotidae) from Japan with notes on its phylogenetic position within the *hufelandi* group. *PLoS ONE* **13**:e0192210. doi:10.1371/journal.pone.0192210.
- Stec D, Gąsiorek P, Morek W, Koszyła P, Zawierucha K, Michno K, Kaczmarek Ł, Prokop ZM, Michalczyk Ł. 2016. Estimating optimal sample size for tardigrade morphometry. *Zool J Linnean Soc* **178**:776–784. doi:10.1111/zoj.12404.
- Stec D, Kristensen RM, Michalczyk Ł. 2018c. Integrative taxonomy identifies *Macrobiotus papei*, a new tardigrade species of the *Macrobiotus hufelandi* complex (Eutardigrada: Macrobiotidae) from the Udzungwa Mountains National Park (Tanzania). *Zootaxa* **4446**:273–291. doi:10.11646/zootaxa.4446.2.7.
- Stec D, Kristensen RM, Michalczyk Ł. 2020c. An integrative description of *Minibiotus ioculator* sp. nov. from the Republic of South Africa with notes on *Minibiotus pentannulatus* Londoño et al., 2017 (Tardigrada: Macrobiotidae). *Zool Anz* **286**:117–134. doi:10.1016/j.jcz.2020.03.007.
- Stec D, Krzywański Ł, Michalczyk Ł. 2018b. Integrative description of *Macrobiotus canaricus* sp. nov. with notes on *M. recens* (Eutardigrada: Macrobiotidae). *Eur J Taxon* **452**:1–36. doi:10.5852/ejt.2018.452.
- Stec D, Krzywański Ł, Zawierucha K, Michalczyk Ł. 2020b. Untangling systematics of the *Paramacrobiotus areolatus* species complex by an integrative redescription of the nominal species for the group, with multilocus phylogeny and species delineation within the genus *Paramacrobiotus*. *Zool J Linnean Soc* **188**(3):694–716. doi:10.1093/zoolinnean/zlz163.
- Stec D, Morek W, Gąsiorek P, Blagden B, Michalczyk Ł. 2017b. Description of *Macrobiotus scoticus* sp. nov. (Tardigrada: Macrobiotidae: *hufelandi* group) from Scotland by means of integrative taxonomy. *Annales Zoologici* **67**:181–197. doi:10.3161/00034541ANZ2017.67.2.001.
- Stec D, Morek W, Gąsiorek P, Michalczyk Ł. 2018a. Unmasking hidden species diversity within the *Ramazzottius oberhaeuseri* complex, with an integrative redescription of the nominal species for the family Ramazzottiidae (Tardigrada: Eutardigrada: Parachela). *Syst Biodivers* **16**(4):357–376. doi:10.1080/1477200.2018.1424267.
- Stec D, Roszkowska M, Kaczmarek Ł, Michalczyk Ł. 2018e. *Paramacrobiotus lachowskiae*, a new species of Tardigrada from Colombia (Eutardigrada: Parachela: Macrobiotidae). *New Zeal J Zool* **45**(1):43–60. doi:10.1080/03014223.2017.1354896.
- Stec D, Smolak R, Kaczmarek Ł, Michalczyk Ł. 2015. An integrative description of *Macrobiotus paulinae* sp. nov. (Tardigrada: Eutardigrada: Macrobiotidae: *hufelandi* group) from Kenya. *Zootaxa* **4052**:501–526. doi:10.11646/zootaxa.4052.5.1.
- Stec D, Tumanov DT, Kristensen RM. 2020a. Integrative taxonomy identifies two new tardigrade species (Eutardigrada: Macrobiotidae) from Greenland. *Eur J Taxon* **614**:1–40. doi:10.5852/ejt.2020.614.
- Stec D, Zawierucha K, Michalczyk Ł. 2017a. An integrative description of *Ramazzottius subanomalous* (Biserov, 1985) (Tardigrada) from Poland. *Zootaxa* **4300**(3):403–420. doi:10.11646/zootaxa.4300.3.4.
- Surmacz B, Morek W, Michalczyk Ł. 2019. What if multiple claw configurations are present in a sample? A case study with the description of *Milnesium pseudotardigradum* sp. nov. (Tardigrada) with unique developmental variability. *Zool Stud* **58**:32. doi:10.6620/ZS.2019.58-32.
- Thulin G. 1928. Über die Phylogenie und das System der Tardigraden. *Hereditas* **11**:207–266.
- Tumanov DV. 2005. Notes on the Tardigrada of Thailand, with a description of *Macrobiotus alekseevi* sp. nov. (Eutardigrada, Macrobiotidae). *Zootaxa* **980**:1–16. doi:10.11646/zootaxa.999.1.1.
- Welnicz W, Grohme MA, Kaczmarek Ł, Schill RO, Frohme M. 2011. ITS-2 and 18S rRNA data from *Macrobiotus polonicus* and *Milnesium tardigradum* (Eutardigrada, Tardigrada). *J Zool Syst Evol Res* **49**:34–39. doi:10.1111/j.1439-0469.2010.00595.x.

Supplementary Materials

Table S1. Raw morphometric data for *Macrobiotus crustulus* sp. nov. (download)

Table S2. Raw morphometric data for *Paramacrobiotus filipi* sp. nov. (download)

Table S3. Uncorrected pairwise distances. (download)